Reviewer 1

> *"My main concerns rest with a need for some increased detail in the Introduction (to strengthen the need to tackle the question they pose) and Methods (at times it feels that the details are rather swiftly handled). I also have some questions around the discussion of differences in the signals recorded on glacial-interglacial timescales and longer term (Pleistocene-Pliocene). My suggestions are provided in more detail below, alongside some minor corrections (typos etc.)"*

We have increased the detail in the introduction (Page 2 lines 12-14) and methods (page 4 lines 18-4, page 5 lines 1-8, page 6 lines 16-17, lines 19-21, line 23, page 7 lines 10-17) and tightened up our use of language surrounding timescales throughout the manuscript.

> *"(1) The Introduction (page 2) makes many statements about 'low' and 'high' CO2 worlds, but no numbers are given. It would be useful to give this context, considering that an expected audience might span Quaternary scientists (for whom an interglacial CO2 might be 'high') and those interested in Cenozoic climate evolution. Either state the known ranges where descriptive terms are used, or consider tabulating some of the studies you cite."*

We now specific enumerate CO_2 levels in the introduction (Page 2 lines 12-14) and have tightened up our language on CO_2 levels throughout the manuscript.

> *"Likewise, on page 2 lines 20-21 there is a note to different earth system sensitivity studies and their 'differences', but it isn't clear whether these are (in)significant, within error etc. Adding some of these details would really help the reader to get a quick sense of whether the problem posed here (different CO2 from different proxies) is something of major importance, or more nuanced and perhaps less critical."*

We've added a further sentence here which now explains the discrepancy (Page 2 lines 21-24)

> *(2) Methods detail. The methods section is well written, but on several occasions some details are missing which would help the reader to follow the flow and/or to understand the rationale for why certain approaches were taken. Specifically:*
>
> *a. page 4 line 11: which alkenone-SST calibration was used? what was the value of modern salinity? The same as stated later for boron isotopes?*
>
> *b. page 4 line 14-15: what were the instrument conditions for the d13C analysis? (GC method, IRMS conditions, reference gases or standards used for d13C ...). Or, less ideally, make reference to the Badger et al. (2013) study but only if the full instrument conditions are clearly stated there.*
>
> *c. page 4 line 14-15: You state where the boron measurements were taken – for consistency can you also say where the d13C was measured?*

We have greatly expanded the Methods section and now include all of these details (Page 4 lines 18 – 24 and 5 lines 1-8).

> *d. page 5 line 5: this range and uncertainty for UK37 and calcite d13C are not explained. Given known non-linearity in the SST calibration at the upper end, and*

the notes of analytical variation in generating SSTs in this study (line 7 on this page), can the authors state whether this range of uncertainty is more than required, or is it instead a realistic estimate when different calibrations and replicates are considered? Later in the manuscript there is a suggestion that 'realistic' values are the focus here, but thatis not obvious from this paragraph.

We have added in an explanatory note about the alkenones earlier in the methods (Page 5 lines 5-7) the calcite d13C uncertainty is a generous estimate based on analytical uncertainty of the measurements.

e. page 5 line 10: state how was the disequilibrium was accounted for, even if it is just a simple step.

This is just a simple subtraction, which we now include in the methods (Page 6 lines 1-2)

f. page 6 line 1: confirm whether these are the same salinity values used for the alkenones (see comment (a) above).

It is, and this is now included (Page 6 line 17, Page 4 line 14)

g. Page 6 line 5: clarify whether these 'Values from Foster' are the reconstructed CO2, or something else (the inorganic chemical constants from the previous sentence?).

These are the reconstructed CO_2 values, which we now state (Page 6 line 23)

(3) Discussion of different timescales. On page 7 (line 17) the authors state that the pCO2 record is "largely stable and invariant ... through both the Pliocene and PLeistocene...". But in Figures 3 and 4 I would argue that there is still variability on orbital (glacial-interglacial timescales) which can be identified in the original alkenone d13C data as well as in the reconstructed pCO2. The apparent stability and lack of variance is instead reflected in the comparison of the longer term data sets i.e. between the Pliocene and Pleistocene, but only for pCO2 (all other measurements do seem to show an offset). This statement on page 7 (line 17) requires some expansion to account for the differences in temporal response i.e. whether there is "a lack of variability". What now becomes intriguing is that not only does pCO2 fail to record Pleistocene glacials, but apparently also Pliocene interglacials, despite offsets being determined in the original alkenone d13C and epsilon-p values.

Although there is variability in the alkenone $\delta^{13}C$ in the Pliocene and the Pleistocene it is not on orbital timescales, and as can be seen in Figures 3 and 4 much of it is within error (especially once it is converted to CO_2). While there are wiggles in the data, these do not match known glacial-interglacial cycles in the Pliocene, and whilst there is a positive slope in Figure 4b, it is not statistically different from zero, as our analysis shows.

a. *page 10 line 24: notes to the possible influence of an incorrect SST calculation on the CO2 calculation. Here, it would be useful to reflect on the uncertainty range used in the original calculations. Would using a different SST calibration yield a better result, especially given the known non-linearities in UK37-SST calibrations at high SSTs?*

We have added a sentence here (page 12 line 14-16) noting that if there is a SST error it would need to be substantial to go beyond what we include in the uncertainty propagation. The Mg/Ca record from Chalk et al., 2017 does not suggest that our alkenone SST is significantly muted (although likely recording a slightly different part of the water column).

> *b. page 11 paragraph 2: parameterisation of physiological factors. The authors note that the dominant alkenone-producing species today is Emiliania huxleyi. But, given the importance of physiological factors suggested here, is it known that E hux has always been present/dominant at this site through the Pleistocene glacial-interglacial cycles? (the cited paper by Winter et al., 2002 is for modern seawater) Is it known which other species might contribute, and if they are closely related? For the Pliocene, this becomes perhaps more crucial: the manuscript does not highlight that in the absence of E hux, there must be a different set of producers in the Pliocene (which could perhaps account for a different relationship between epsilon-p and CO2?). Is there any information from this site about which coccolithophore species are present in the Pliocene and through the Pleistocene? If there isn't, then it would still be useful to state this as an uncertainty. Have the authors looked at alkenone accumulation rates as a possible indicator of export flux (and potentially productivity) to see if there are any glacial-interglacial or Pliocene-Pleistocene differences?*

Emiliania huxleyi coccoliths are first recognised in the fossil record at around 290 Ka, and take over as the dominant species in the ocean at around 82 Ka (Raffi et al., 2006) we now include this reference which was missed out), prior to this the closely related *Gephyrocapsa oceanica* (or related species) dominated, and was likely the major alkenone producer (Raffi et al., 2006). Most of our Pleistocene record therefore probably represents alkenones produced by *Gephyrocapsa* spp*.,* whilst the Pliocene record is likely another closely related noelaerhabdaceae such as *Reticulofenestra*. We cannot therefore rule out these different species having different species having different physiological responses (although note that they are very closely related species of the same family and likely occupied a similar niche) and now include a sentence to that effect (page 13 lines 10-17). We do however note that the nearby Site 925 record is similarly invariant through the last glacial-interglacial cycle, and would have been produced entirely by *E. huxleyi*, and so this change in species cannot be the complete explanation.

> *Minor corrections*
>
> *- Format UK37' with the correct sub/superscript throughout*

Done.

> *- page 7 line 16 – comment about glacial temperatures: no comment made about the, unusually cold SST which isn't in the glacial*

This is likely just an outlier and so we have chosen not to discuss it in detail.

> *- page 6 line 11 – explain how "using alkenones limits the variation of cell geometry"... aren't alkenones synthesised by multiple species of haptophyte, which could have different cell geometries? Any citation for support?*

Using alkenones rather than other biomarkers or bulk organic matter to calculate ε_p restricts source organisms to the very limited group of haptophytes that produce alkenones, this excludes organic

matter produced by organisms such as diatoms, radiolarians and dinoflagelates (for example) which have a much greater range of cell geometries. This is covered in Popp et al., (1998) and Laws et al., (1997) and we have now moved that reference from earlier in the sentence to make that clear (page 7 line 4)

> *- page 7 lines 18-20 – this information about estimating 'b' seems out of place here, and interrupts the flow. Better in the methods section, or in the paragraph which follows where the differences to Seki can be outlined?*

This is already included in the methods section (page 5 line 15) so we have removed the sentence here to improve the flow.

> *- page 10 line 15 – "and test which variables maybe responsible" ?*

Done (page 12 line 4)

> *- page 10 line 16 – "largely invariant for the Pleistocene ..."?*

Done (page 12 line 5)

> *- add analytical uncertainty bars to Figure Panels 3a and 3e (or state if these are too small to be seen)*

Done.

> *- why are figures 3 and 4 showing different width of time for pliocene? Please can figure 3 show the pliocene data as well (which is shown in figures 2 and 4?)*

These figures show the new data, the remainder of the Pliocene data was published in Badger et al., (2013).

> *- caption figure 4 – isnt lith size panels a and d? Clarify that the drop in lith size (page 9 lines 12-15) is reflected in mean/median (figure 4?), since there doesn't seem to be any shift in the ranges between the two time intervals.*

The caption and sentence (page 10 line 19) has been changed.

Reviewer 2

> *My only substantial comment is that I think the authors should calculate the Pliocene pCO2 values from the alkenone proxy with the cell size corrections added (and do the same for the Pleistocene samples for comparison). I realize this doesn't change the orbital-scale insensitivity in the Pleistocene. But, it does allow comparison of the absolute value and magnitude of change between the Pleistocene and Pliocene windows in both proxies. It will also change the posterior distributions of the input variables for the alkenone pCO2 reconstructions. My sense is that it will bring the b-parameter, ef, and SST posteriors more in line with the priors. The lith size changes are on the order of 150 to 200% higher in the Pliocene with respect to the Pleistocene (it appears from the figure). That is substantial and would increase the estimated Pliocene pCO2 values into the high 300 to low 400 ppm range – very similar to the 11B pCO2 estimates. This may indicate that the alkenone pCO2 proxy agrees in magnitude with Plio-Pleistocene pCO2 changes and thus may be sensitive at higher CO2 levels but not at the very low Pleistocene glacial levels. The authors suggest this might be the case in the conclusions. If they show it is the case with their Pliocene reconstructions it would provide some nice empirical support (and they should mention this in the abstract).*

We chose not to build the lith size correction into our Bayesian approach because the correction, following Henderiks and Pagani (2007) and Seki et al. (2010) involves some rather arbitrary scaling. This is because the correction results in very low CO_2 during the Pleistocene compared to the ice core (Figure 6 panel c). If we follow Seki et al. (2010) and scale b' so that the ice core interval is correct and then apply this same scaling of b' to the Pliocene interval then, as the reviewer predicted, we do see a good overlap between the boron and the alkenone (new Figure 6). Although it should be noted that this correction does not induce glacial-interglacial cyclicity in the Pleistocene alkenone data. To more empirically examine if cell-size played a role in the differences as the reviewer suggests, but to also avoid the arbitrary nature of the cell-size correction which is difficult to enact in a Bayesian sense, we now include a figure showing lith size vs. posterior b (Figure 11). This shows that there is a good correlation between b and lith size ($R^2 = 0.52$, $p<<0.01$) but it is quite different to the relationship predicted by Hendriks and Pagani (2007) shown by the green dot-dash line in the Figure. This suggests that if cell-size is important, its influence on b is not as we currently understand it. We now add these two figures figure and text to this effect in the revised manuscript (Figure 6, Figure 11, page 7 lines 10-17, page 13, lines 1-6).

> *Page 4 line 15 – how were alkenone 13C isotope measurements calibrated and what was the replicate precision and the accuracy (i.e. uncertainty from analysis plus uncertainty in realizing the VPDB scale). (Same comment for p5 line 6).*

We've now substantially expanded the methods section (page 4 lines 20-24, page 5 lines 1-8) and include this information there.

> *Page 9 line 20 – The previous paragraph stated that there is some evidence for a reduction in productivity during glacials and if that translates to cell-specific growth rates then it could explain some of the lack of signal in the alkenone pCO2 reconstructions. In light of that observation, the following statement is confusing to me: "This suggests that either our understanding of growth rate effects on CO2("p-alk) is incorrect, or the estimation of cell size using preserved liths does ot*

capture original cell size variations: : :." Doesn't the prior statement suggest that our understanding of growth rate effects may actually be correct?

Our point in the previous paragraph is that growth rates could be part of the story (if the evidence of low productivity is correct) but that the scale of change required the move the reconstructed $CO_{2(\varepsilon p\text{-}alk)}$ in line with the $CO_{2(\delta 11Bplank)}$ and ice core CO_2 for the glacial is very substantial (see Figure 1), and greater than we think likely based on our current understanding of how growth rates would effect ε_p, This suggests to us that if growth rate is the main cause for the discrepancy our understanding of growth rate effects on ε_p is incorrect. We have added text to explain this (page 11 line 5-6).

Page 10 line 25 – This paragraph is quite instructive, nice! One question is how the SST posterior is calculated? For the Pliocene, the SST would also affect the pCO2 estimated by the 11B method. Thus, if one assumes a pCO2 from the 11B and then gets a posterior SST from the alkenone proxy, this different SST would change the 11B pCO2 estimate and thus the alkenone SST posterior based upon the earlier 11B CO2 value is no longer correct.

This is potentially correct, but we chose not to do this for two reasons, 1) the temperature effect on $CO_{2(\delta 11Bplank)}$ is actually fairly minor (less so than $CO_{2(\varepsilon p\text{-}alk)}$) and 2) as we use different SST records for $CO_{2(\varepsilon p\text{-}alk)}$ and $CO_{2(\delta 11Bplank)}$ ($U_{37}^{K'}$ for the former and Mg/Ca in planktic foraminifera for the latter) to keep the carrier organisms the same, producing a sutiable SST for the $CO_{2(\delta 11Bplank)}$ would be non-trivial.

Page 11 line 5 – ": : :the current understanding of the CO2(ep-alk) proxy is wanting." Yes, the b term may not in fact capture the scaling of physiological parameters or the truly important parameters.

Although this may not have been the reviewers intention, we have lifted this nice phrasing almost in it's entirety and added it at page 12 line 21-2, we hope they don't mind!

Page 11 line 19 – The sentence starting, "Additionally, CO2 optima: : :" is a bit unclear. I think the authors are saying that different species have different CO2 optima so that CCM effects may vary between regions where different species dominate? But maybe not that. Please rewrite and clarify.

We've restructured this sentence (page 14 lines 3-5) which is now hopefully clearer.

Additionally, following correspondence prompted by the publication of the discussion paper, we now improve the clarity and robustness of our citation of the ice core data with the addition of Table 1, and changed the discussion of other $CO_{2(\varepsilon p\text{-}alk)}$ records from the Pleistocene to better represent the intent of some of those works (page 11 lines 11-20).

Insensitivity of alkenone carbon isotopes to atmospheric CO_2 at low to moderate CO_2 levels

Marcus P.S. Badger*[1,2], Thomas B. Chalk[3,4], Gavin L. Foster[3], Paul R. Bown[5], Samantha J. Gibbs[3], Philip F. Sexton[1], Daniela N. Schmidt[6,7], Heiko Pälike[8], Andreas Mackensen[9] and Richard D. Pancost[2,7]

[1]School of Environment, Earth & Ecosystem Sciences, The Open University, Milton Keynes, MK7 6AA, UK
[2]Organic Geochemistry Unit, School of Chemistry, School of Earth Sciences, University of Bristol, Bristol, BS8 1TS, UK
[3]School of Ocean and Earth Science, National Oceanography Centre Southampton, University of Southampton, Southampton SO14 3ZH, UK
[4]Department of Physical Oceanography, Woods Hole Oceanographic Institution, Woods Hole, MA, 02543, USA
[5]Department of Earth Sciences, University College London, London, WC1E 6BT, UK
[6]School of Earth Sciences, University of Bristol, Wills Memorial Building, Queens Road, Bristol, BS8 1RJ, UK
[7]The Cabot Institute, University of Bristol, Bristol BS8 1UJ, UK
[8]MARUM – Center for Marine Environmental Sciences, University of Bremen, Bremen, Germany
[9]Alfred Wegener Institute for Polar and Marine Research, Am Alten Hafen 26, 27568 Bremerhaven, Germany

Correspondence to: Marcus P.S. Badger (marcus.badger@open.ac.uk)

Abstract Atmospheric pCO_2 is a critical component of the global carbon system and is considered to be the major control of Earth's past, present and future climate. Accurate and precise reconstructions of its concentration through geological time are, therefore, crucial to our understanding of the Earth system. Ice core records document pCO_2 for the past 800 kyrs, but at no point during this interval were CO_2 levels higher than today. Interpretation of older pCO_2 has been hampered by discrepancies during some time intervals between two of the main ocean-based proxy methods used to reconstruct pCO_2: the carbon isotope fractionation that occurs during photosynthesis as recorded by haptophyte biomarkers (alkenones) and the boron isotope composition ($\delta^{11}B$) of foraminifer shells. Here we present alkenone and $\delta^{11}B$-based pCO_2 reconstructions generated from the same samples from the Pliocene and across a Pleistocene glacial-interglacial cycle at ODP Site 999. ~~across a glacial-interglacial cycle.~~ We find a muted response to pCO_2 in the alkenone record compared to contemporaneous ice core and $\delta^{11}B$ records, suggesting caution in the interpretation of alkenone-based records at low pCO_2 levels. This is possibly caused by the physiology of CO_2 uptake in the haptophytes. Our new understanding resolves some of the inconsistencies between the proxies and highlights that caution may be required when interpreting alkenone-based reconstructions of pCO_2.

1. **Introduction**

Understanding the absolute level and evolution of atmospheric pCO_2 through geological time is essential to our understanding of the Earth's Climate System. As both a fundamental, first order control, and a contributor to multiple dynamic feedbacks, atmospheric pCO_2 is critical in setting Earth's surface temperature (Lacis et al., 2010). Reconstructing pCO_2 evolution improves the understanding of both the mechanisms behind past climate change (Chalk et al., 2017) , and provides novel constraints on climate sensitivities (Martínez-Botí et al., 2015; PALAEOSENS, 2012). This then allows ground-truthing of our understanding the climate and the Earth system models that are used for predicting future climate change.

Over the past two decades, two common marine-based CO_2 proxies have emerged – alkenone-based ε_p values ($CO_{2(\varepsilon p\text{-}alk)}$), utilising the carbon isotopic fractionation imparted during photosynthesis in a subgroup of haptophytes (Bidigare et al., 1997), and planktic foraminiferal $\delta^{11}B$ values ($CO_{2(\delta 11Bplank)}$), based on the pH control of boron speciation and isotopic fractionation in seawater (Hemming and Hanson, 1992). Multiple records of atmospheric pCO_2 now exist for the Cenozoic from both methods, showing a broadly similar long-term trend from a high-CO_2 greenhouse world of the early Cenozoic when CO_2 exceeded 400 µatm and may have been as higher than 1000 µatm to a low-CO_2 bi-polar glaciated world of the ~~present~~ late Pleistocene, when CO_2 fell to below 300 µatm (Anagnostou et al., 2016; Foster et al., 2017; Pagani et al., 2005, 2011; Pearson et al., 2009; Sosdian et al., 2018; Super et al., 2018).

However, discrepancies have recently become apparent between both methods when applied to the last 20 Ma (Badger et al., 2013a, 2013b). Specifically, the $CO_{2(\varepsilon p\text{-}alk)}$ reconstructions often suggest a lower magnitude of short-term pCO_2 change compared to that from $CO_{2(\delta 11Bplank)}$ (Badger et al., 2013a). Whilst this could be partially explained by mismatches between the sampling intervals, or by the influence of local surface water disequilibrium with the atmosphere with respect to CO_2, this discrepancy remains even for records generated from exactly the same sediment samples (Badger et al., 2013b vs Martínez-Botí et al., 2015). Both the $CO_{2(\varepsilon p\text{-}alk)}$ and $CO_{2(\delta 11Bplank)}$ have been used to estimate Earth system sensitivity in the Pliocene ~~(e.g. Pagani et al., (2009) vs. Martínez-Botí et al., (2015))~~ with differing results; $CO_{2(\varepsilon p\text{-}alk)}$ suggesting higher than present earth system sensitivity Pliocene (7-10 °C per CO_2 doubling; Pagani et al., 2009), whilst $CO_{2(\delta 11Bplank)}$ records sensitivity in line with our estimates for today (<5 °C per CO_2 doubling; Martínez-Botí et al., 2015).~~; a~~Although this is at least partly due to the

different approaches used to calculate Earth system sensitivity in the two studies, it is also due to the differences in reconstructed pCO_2 from the two approaches.

The $CO_{2(\varepsilon p\text{-}alk)}$ and $CO_{2(\delta 11Bplank)}$ palaeobarometers are both based on mechanistic frameworks that have been calibrated in either the modern ocean or laboratory culture (Bidigare et al., 1997; Hemming and Hanson, 1992; Pagani et al., 2002; Sanyal and Hemming, 1996). These proxies can be further ground-truthed in the recent geological past, when ice core records provide high-quality pCO_2 data for the last 800 kyrs (Bereiter et al., 2015 and Table 1). In previous work, both $CO_{2(\delta 11Bplank)}$ (Chalk et al., 2017; Foster, 2008; Foster and Sexton, 2014; Henehan et al., 2013; Hönisch and Hemming, 2005; Sanyal et al., 1995) and $CO_{2(\varepsilon p\text{-}alk)}$ (Jasper and Hayes, 1990) yield pCO_2 records similar in absolute value and amplitude of change to those derived from ice cores. However, the emerging discrepancies between the two methods (Badger et al., 2013a, 2013b; Martínez-Botí et al., 2015~~b~~) necessitate revisiting this validation, both between the two proxies, and between marine proxy and ice core reconstructions.

The ice core records pCO_2 of the Pleistocene glacial-interglacial cycles (Bereiter et al., 2015 and Table 1~~; Petit et al., 1999~~) provide an opportunity for cross-calibrating proxy methods for determining atmospheric pCO_2 in the geological archive ($CO_{2(\varepsilon p\text{-}alk)}$ and $CO_{2(\delta 11Bplank)}$) with the direct-CO_2 measurements from the ice cores.

1.2 Study Site

Ocean Drilling Program Site 999 is located in the Caribbean Sea (12° 44.639' N, 78° 44.360' W, 2838m water depth; Figure 1), has an orbitally calibrated age model and has been used previously for CO_2 reconstructions. Our temporal sampling resolution is ~6 kyrs in the Pleistocene and ~9 kyrs in the Pliocene. Although $CO_{2(\varepsilon p\text{-}alk)}$ and $CO_{2(\delta 11Bplank)}$ are independent of one another in many respects, they both rely on assumptions about the equilibrium of surface seawater with the atmosphere with respect to CO_2, sea surface temperature, and on well-constrained age models, which can make direct comparison between records from different sites difficult. Here we overcome these problems by producing $CO_{2(\varepsilon p\text{-}alk)}$ and $CO_{2(\delta 11Bplank)}$ records from identical horizons in the same deep ocean sediment core in 1) the late Pleistocene, permitting direct comparison to ice core data (Figure 2a, Figure 3), and 2) across the intensification of Northern Hemisphere glaciation (INHG) in the Pliocene (Martínez-Botí et al., 2015~~a~~; Seki et al., 2010) (Figure 2b).

In terms of CO_2, ODP Site 999 in the Caribbean Sea is today slightly out of equilibrium with the atmosphere, with surface waters a little oversaturated in CO_2, providing a small net source of CO_2 to the atmosphere (~21 µatm; Takahashi et al., 2009). However the site has been shown to be suitable for recording past changes in pCO_2 (Foster, 2008; Foster and Sexton, 2014) and the air-sea equilibrium is not thought to have changed significantly from the Pliocene to today (see discussion in Bartoli et al., 2011). It is one of few sites where both alkenone and boron isotope records can be acquired given the good preservation of both foraminifera and organic matter (Badger et al., 2013b; Foster, 2008; Foster and Sexton, 2014; Martínez-Botí et al., 2015~~a~~), and Pliocene records of both are available (Badger et al., 2013b; Bartoli et al., 2011; Martínez-Botí et al., 2015~~a~~). It also has been demonstrated previously to record glacial-interglacial cycles of pH/CO_2 (Foster, 2008; Henehan et al., 2013) and a Pleistocene $CO_{2(\delta 11Bplank)}$ record from 0-250 ka has been recently published (Chalk et al., 2017).

2 Methods

2.1 Alkenone isotopes

Our new alkenone based CO_2 record was calculated following Badger et al., (2013b), with modern day phosphate used in the estimation of the 'b' term, $U_{37}^{K'}$ ~~*UK37*~~' temperatures, and modern day salinity (35 psu). Samples were freeze dried, ground to a fine powder by hand, and extracted by Soxhlet apparatus using a dichloromethane (DCM) / methanol azeotrope (2:1, *v/v*) refluxing for 24 hours. Total lipid extracts were divided into three fractions (F) by small (4 cm) silica chromatography columns, with fractions eluting in 3 mL of *n*-hexane (F1), DCM (F2) and ethyl acetate/*n*-hexane (1:3. *v:v*, F3) respectively. Alkenones eluted in F2. Alkenone identification was confirmed by GC mass spectrometry (ThermoQuest Trace MS, He carrier gas) Alkenone isotope analyses were performed using a ThemoFisher Delta V connected via a Gas Chromatograph (GC) isolink and ConFlo IV to a Trace GC. The GC oven was programmed to increase in temperature from 70 °C to 200 °C at 20 °C min^{-1}, then to 300 °C at 6 °C min^{-1} and held isothemal for 25 min. Conversion to VPDB was performed by reference to a laboratory standard gas of known $\delta^{13}C$ and system performance was monitored using in-house fatty acid methyl ester and *n*-alkane standard mixtures of known isotopic composition. Long term precision is approximately 0.3 ‰. To estimate SST, the F2 fraction was also analysed by GC- flame ionisation detection (Hewlett Packard 5890 Series II), the GC oven was programmed

to increase in temperature from 70 °C to 130 °C at 20 °C min^{-1}, then to 300 °C at 4 °C min^{-1} and held isothermal for 25 min. An approximately 50 m, 0.32 mm internal diameter capillary column with a 0.12 µm thick dimethylpolysiloxane equivalent film. A H_2 carrier gas was used, and quantification was monitored using an hexandecan-2-ol standard added prior to column chromatography. System performance as monitored with an in-house fatty acid methy ester standard. Alkenone ratios were converted to SST using the global core-top calibration of (Müller et al., (1998), although this is a linear calibration, our uncertainty treatment (see below) should encompass any minor deviation from linear as $U_{37}^{K'}$ approaches 1 (see also the discussion in (Badger et al., (2013b). All alkenone analyses were carried out at the Bristol node of the of the NERC Life Sciences Mass Spectrometry Facility hosted by the Organic Geochemistry Unit, University of Bristol.

The alkenone isotope $\delta^{13}C$ value is used to calculate the total carbon isotope fractionation that occurs during algal growth (ε_p). This isotopic fractionation has been shown to be controlled by $[CO_2]_{(aq)}$ (equation 1; Jasper & Hayes 1990) which can then be converted to atmospheric CO_2 using Henry's law.

Equation 1. $$\varepsilon_p = \varepsilon_f - \frac{b}{[CO_2]_{(aq)}}$$

To calculate ε_p from alkenone $\delta^{13}C$ vales the carbon isotopic composition of DIC is required, this is calculated from planktic foraminiferal calcite $\delta^{13}C$, whilst the fractionation which occurs during carbon fixation (ε_f), is here assumed constant. The'b' term is the sum of other physiological factors (such as growth rate, and cell size, and light limitation) which is estimated from the relationship shown in the modern ocean between 'b' and dissolved reactive phosphate $[PO_4^{3-}]$. Further details of the treatment can is detailed in Badger et al., (2013b).

Error bars in relevant figures are all 1sd and based on a full Monte Carlo propagation (n=10000) of the following uncertainties: ±2 °C and ±0.1 ‰ were applied to temperature and foraminiferal calcite $\delta^{13}C$, (normal probability function (pdf), 2σ error) and ±2 and ±0.1 to salinity and $[PO_4^{3-}]$, respectively (2σ; uniform pdf). Uncertainties on alkenone $\delta^{13}C$ were estimated from replicate runs and calcite $\delta^{13}C$ from repeat runs of an internal standard. Integrated analytical and calibration uncertainties for alkenone based temperatures were estimated and conservative estimates of likely variation for salinity and $[PO_4^{3-}]$ were used. An 11 % error on the slope of $b=a[PO_4^{3-}]+c$ was assumed, where a = 116.96 and c = 81.41 (Pagani et al., 1999).

For consistency with the $CO_{2(\delta 11Bplank)}$ record for this Site, we now adjust for the disequilibrium by subtracting the present day CO_2 surplus, and thus, have recalculated the included values of Badger et al., (2013b) accordingly. SSTs for our new Pliocene data were published in Davis et al., (2013).

2.2 Boron Isotopes

Boron isotope data were published in (Chalk et al., 2017) and are from the same core samples as our alkenone measurements. *Globigerinoides ruber sensu stricto* (white, n ~ 200 individuals from 300-355µm) samples were measured for boron isotope composition on Thermo Scientific Neptune MC-ICPMS at the University of Southampton according to methods described elsewhere (Foster et al., 2013; Martínez-Botí et al., 2015~~a~~; Rae et al., 2011). Analytical uncertainty is given by the external reproducibility of repeat analyses of Japanese Geological Survey Porites coral standard (JCP) at the University of Southampton following Henehan et al., (2013) and is typically <0.2 ‰ (at 95 % confidence). Metal element:calcium ratios (Li, Mg, B, Na, Al, Mn, Ba, Sr, Cd, U, Nd, and Fe) were analyzed using an Thermo Element 2XR ICP-MS at the University of Southampton). Here, these data are used to assess adequacy of clay removal (Al/Ca <100 µmol/mol) and to generate down core temperature. pH and CO_2 were calculated using a Monte Carlo approach (uncertainties are 2sd, n = 10000 replicates) using R (R Core Team, 2015), for pH we use a boron isotopic composition of seawater of 39.6 ‰ (2sd of 0.1, Foster et al. 2010) and experimentally determined isotopic fractionation factor (1.027, Klochko et al., 2006) as well as the species specific calibration for *G. ruber* of Henehan et al 2013 (also with incorporated uncertainties). For the CO_2 calculations we use a range of salinity (equal to used in the $CO_{2(\varepsilon p\text{-}alk)}$ calculations) and total alkalinity (Talk) that encompasses the modern values (34-37 and 2100-2500 µM, respectively, both with a uniform rather than normal probability distribution. Temperature was determined using Mg/Ca of *G. ruber* following established methods (Delaney and Boyle, 1985; Evans and Müller, 2012)). Mg/Ca SST of planktic foraminifera is used for $CO_{2(\delta 11Bplank)}$ and alkenone $U^{K'}_{37}$ for $CO_{2(\varepsilon p\text{-}alk)}$ so that the carrier organisms for the CO_2 reconstruction and SST measurements match, ensuring the temperature measurement is coming from the appropriate part of the water column. Inorganic chemical constants were used from the seacarb package in R (Gattuso et al., 2015), and using published values for the pKB (Dickson, 1990). Reconstructed atmospheric CO_2 v~~V~~alues from Foster, (2008) were recalculated to match this approach. All uncertainties are included in our simulation and are roughly equivalent to those assumed for the alkenone data and are exactly the same as those used for Martinez-Boti et al. 2015 excluding the $\delta^{11}B_{sw}$, thus providing a fair comparison.

2.3 Coccolith length measurements

The uptake of CO_2 into the coccolithophore cell is effected by the cell size and geometry ~~(Laws et al., 1997; Popp et al., 1998)~~, using alkenones limits the variation of cell geometry by restricting the source organism to one with exclusively spherical cells (Laws et al., 1997; Popp et al., 1998), but some change in cell size is possible. Coccolith size is used as an semi-quantitative proxy for cell size because coccolith size is typically larger on larger cells, with that relationship being broadly consistent within a single taxonomic group where growth behaviour is broadly comparable (Gibbs et al., 2013; Henderiks, 2008; Sheward et al., 2017). Long-axis coccolith length measurements were therefore taken from 100 specimens of the family Noelaerhabdaceae per sample from standard smear slides. Specimens were imaged at 1500x magnification and measured using CellD software.

To investigate the potential influence of changing cell size on $CO_{2(\varepsilon p\text{-}alk)}$ Equation 1 can be adapted:

Equation 2 $$\varepsilon_p = \varepsilon_f - \frac{b\prime}{[CO_2]_{(aq)}}$$

With b' calculated from using the volume to surface area ratio (V:SA) of modern and fossil coccospheres (Equation 3; Henderiks and Pagani, 2007)

Equation 3 $$b' = b\frac{V{:}SA_{fossil}}{V{:}SA_{Ehux}}$$

$V{:}SA_{Ehux}$ is 0.9 ±0.1 µm in modern haptophytes (Popp et al., 1998) and $V{:}SA_{fossil}$ can be estimated from lith size measurements (Equation 4; Henderiks and Pagani, 2007)

Equation 4 $$D_{cell} = 0.55 + 0.88L_{coccolith}$$

2.4 Age Model

For the interval 0-500 ka, we generated a detailed age model by tuning the planktic foraminifer (*G. ruber*) $\delta^{18}O$ record from Site 999 (at ~0.5 to 2.0 kyr resolution) (Schmidt et al., 2006) to the LR04 benthic $\delta^{18}O$ stack (Lisiecki and Raymo, 2005) using the Analyseries software (Paillard et al., 1996), the Pliocene portion of Site 999 is part the LR04 stack and that astronomically tuned age model is used here (Lisiecki and Raymo, 2005).

2.5 Bayesian exploration of $CO_{2(\varepsilon p\text{-}alk)}$ input variables

In order to examine the influence of the various input parameters for the calculation of pCO_2 from alkenone $\delta^{13}C$ values, we carry out a second set of Monte Carlo simulations (n=100,000) with expanded uncertainty. In this case, we more fully explore uncertainty space using the following input uncertainties (at 95 % confidence or full range): SST (normal distribution, ± 6 °C), ε_f (uniform distribution, 24 to 28), b (normal distribution, ± 40), CO_2 disequilibrium (20 ± 20). These input distributions are our *prior* distributions. We then evaluate the CO_2 output for each alkenone sample against synchronous ice core pCO_2 and boron isotope pCO_2 for the Pleistocene and Pliocene, respectively. By only selecting those simulated alkenone pCO_2 levels that agree with ice core or $pCO_{2(\delta 11Bplank)}$ (including associated uncertainties), we can re-evaluate the input distributions (our *posterior*) and gain insights into the relative importance of each of the input variables in potentially driving the observed disagreements in pCO_2. Uncertainties in the $pCO_{2(\delta 11Bplank)}$ are as described above, and we apply an uncertainty of ± 6 ppm (2s) for the ice core pCO_2 record (Ahn et al., 2012).

3 Results and Discussion

Alkenone and *G. ruber* $\delta^{13}C$ values (Figure 3a,e) were used to calculate ε_p values (Figure 3c,g). Alkenone $\delta^{13}C$ values are relatively stable through the Pleistocene portion of the record, varying between -24.5 ‰ and -23.2 ‰. Values are slightly higher in the Pliocene, varying between -24.1 ‰ and -21.7 ‰, *G. ruber* $\delta^{13}C$ values are relatively stable through the whole record, varying between 0.53 ‰ and 1.57 ‰. These give rise to ε_p values which are similarly fairly stable, varying between 10.5 ‰ and 12.2 ‰ in the Pleistocene, and between 9.53 ‰ and 11.8 ‰ in the Pliocene. Our $U_{37}^{K'}$ ~~UK37'~~ SST (Figure 3c,g) record shows warmer temperatures in the Pliocene of around 27 °C, with cooler temperatures recorded in the Pleistocene, with the coldest SST recorded in the glacial which is ~2 °C cooler than the interglacial. These record are combined (see Methods)

to produce the pCO_2 record (Figure 2, 3c,f) which shows largely stable and invariant values through both the Pliocene and Pleistocene portions of our record. ~~We estimate the 'b' term of equation 1 using the modern day relationship observed between 'b' and $[PO_4^{3-}]$. This term combines all other physiological factors which may influence ε_p including cell size, growth rate and light limitation.~~

Published low temporal resolution Pliocene records from Site 999 (Seki et al., 2010), using both the $CO_{2(\varepsilon p\text{-}alk)}$ and $CO_{2(\delta 11Bplank)}$ palaeobarometers, show a pCO_2 decrease at ~ 2.8 Ma. However, this agreement relies on correcting the $CO_{2(\varepsilon p\text{-}alk)}$ for changes in haptophyte cell size, which was based on a low temporal resolution lith size record (Seki et al., 2010). Changes in haptophyte cell size alter the volume:surface area ratio available for gaseous exchange, and can therefore modify the fractionation recorded by $CO_{2(\varepsilon p\text{-}alk)}$(Popp et al., 1998). Our new $CO_{2(\varepsilon p\text{-}alk)}$ record at Site 999 now spans 3.3- 2.6 Ma at higher temporal resolution, supplementing data from Badger et al., (2013b). A lith size record has also been generated for the same samples used for $CO_{2(\varepsilon p\text{-}alk)}$ for 3.3-2.6 Ma (Davis et al., 2013). We find no evidence to support the change in lith size applied by Seki et al., (2010) with lith size (and hence cell size) remaining stable across the primary pCO_2 change at 2.8 Ma (Davis et al., 2013). Consequently, although our new $CO_{2(\varepsilon p\text{-}alk)}$ record is higher resolution than that of Seki et al., (2010), we no longer have any evidence for the cell size shift at 2.7 Ma (Figure 4).

We compare our record with the $CO_{2(\delta 11Bplank)}$ records of Martínez-Botí et al., (2015) in Figure 2. With the cell size correction now removed, the decrease in $CO_{2(\varepsilon p\text{-}alk)}$ across the INHG, and the agreement of $CO_{2(\varepsilon p\text{-}alk)}$ with $CO_{2(\delta 11Bplank)}$, both now disappear (red symbols, Figure 2b). As such, $CO_{2(\varepsilon p\text{-}alk)}$ for the whole of this Pliocene interval (2.6 – 3.3 Ma) remains stable and low (mean $CO_{2\,(\varepsilon p\text{-}alk)}$ =251±13; 1σ min=228 max=286 μatm), whereas $CO_{2(\delta 11Bplank)}$ is on average higher and more variable (mean $CO2_{(\delta 11Bplank)}$=342±50; 1σ min=234 max=452 μatm).

In the Pleistocene, our $CO_{2(\varepsilon p\text{-}alk)}$ record covers one complete glacial-interglacial (G-IG) cycle from 110 – 260 ka, encompassing Marine Isotope Stage (MIS) 5,6,7 the end of MIS 8, and terminations II and III (red open diamonds, Figure 2a). The $CO_{2(\delta 11Bplank)}$ record of Chalk et al. (2017) covers two G-IG cycles from the late Holocene to MIS8 (blue open circles, Figure 2a). $\delta^{11}B_{plank}$ closely tracks the rise and fall of pCO_2 derived from ice cores (Chalk et al., 2017), with $CO_{2(\delta 11Bplank)}$ exhibiting similar values to atmospheric CO_2 within uncertainty (Figure 2a), and with only small deviations from ice core CO_2 as a result

of: (*i*) the noise in the reconstruction; and (*ii*) perhaps a small diagenetic effect on $CO_{2(\delta 11Bplank)}$ relating to periods of carbonate dissolution in portions of the core which show high foraminiferal fragmentation (e.g. MIS 5d; Schmidt et al., 2006).

In contrast, $CO_{2(\varepsilon p\text{-}alk)}$ is within error of the ice core data only during the interglacials when CO_2 partial pressures are similar to those of the pre-industrial era. Crucially, $CO_{2(\varepsilon p\text{-}alk)}$ clearly fails to record the lower pCO_2 of the glacials, remaining at around 260 μatm throughout (mean $CO_{2(\varepsilon p\text{-}alk)}$=259±27; Figure 2a). This concentration of pCO_2 is also very close to that recorded by $CO_{2(\varepsilon p\text{-}alk)}$ in the Pliocene at this Site (mean $CO_{2(\varepsilon p\text{-}alk)}$=252±26 μatm; Figure 2). Similar alkenone behaviour has also been observed in another, albeit lower resolution, record from ODP Site 925 (Zhang et al., 2013; Figure 2), where the $CO_{2(\varepsilon p\text{-}alk)}$ remains unchanged during the Pleistocene (20 – 170 Ka) and Pliocene.

Overall, these results suggest that, at least at these sites, the $CO_{2(\delta 11Bplank)}$ palaeobarometer does faithfully record atmospheric CO_2 change, whereas the $CO_{2(\varepsilon p\text{-}alk)}$ proxy is unable to reconstruct the low levels of atmospheric CO_2 during the glacial. This suggests that, in its present and frequently applied form, $CO_{2(\varepsilon p\text{-}alk)}$ is not accurately recording atmospheric CO_2, and this could explain the discrepancy between the Pliocene $CO_{2(\varepsilon p\text{-}alk)}$ and $CO_{2(\delta 11Bplank)}$ records. We further evaluate this by using regression analysis between ice core and the paired-proxy data (Figure 5). $CO_{2(\delta 11Bplank)}$ levels are largely consistent with those determined from ice cores, clustering around the 1:1 line with a slope also close to 1 (0.95±0.13) (Figure 5a), whereas variance in $CO_{2(\varepsilon p\text{-}alk)}$ is strongly muted compared to that observed in the ice core data (Figure 5b).

As both cell size (Popp et al., 1998) and growth rate (Bidigare et al., 1997) can modify $\delta^{13}C_{alk}$ via the 'b' term, we investigated whether either of these could explain the muted response of $CO_{2(\varepsilon p\text{-}alk)}$ to atmospheric CO_2. Hapytophyte cell size can be estimated from their lith size, but as noted above, there is no evidence for significant changes in the Pliocene (Davis et al., 2013) nor is there evidence for any change across MIS5-8 (Figure 4a). There is an overall reduction in mean lith size from the Pliocene to the Pleistocene (Figure 4a, b), which could offset a long term pCO_2 decline and thus explain the apparent lack of difference between Pliocene and Pleistocene $CO_{2(\varepsilon p\text{-}alk)}$ at Site 999 (Figure 6). However, this longer-term reduction in lith size cannot explain the muted response to Pleistocene G-IG CO_2 change.

Growth rate is more difficult to reconstruct; most available proxy systems reconstruct phytoplankton or whole ecosystem productivity, rather than coccolithophorid growth rate. However emerging trace metal datasets do suggest changing productivity on glacial-interglacial timescales at Site 999, with lower productivity in the glacial (Trumbo, 2015). If lower productivity is linked with a simultaneous reduction in growth rate, then it could explain some of the lack of signal in $CO_{2(\varepsilon p\text{-}alk)}$, however to reduce the $CO_{2(\varepsilon p\text{-}alk)}$ sufficiently to overlap with ice core CO_2 would require an order of magnitude reduction in growth rates during the glacial. ~~.~~

This suggests that either our understanding of growth rate effects on $CO_{2(\varepsilon p\text{-}alk)}$ is incorrect, or the estimation of cell size using preserved liths does not capture original cell size variations, or a combination of these or other factors leads to the rather muted trends in $CO_{2(\varepsilon p\text{-}alk)}$ through the glacial-interglacial cycle.

The failure of $CO_{2(\varepsilon p\text{-}alk)}$ from these two sites to record the G-IG pCO_2 variation also necessitates reassessment of earlier $CO_{2(\varepsilon p\text{-}alk)}$ studies that were able to reconstruct such changes. For instance whilst Jasper and Hayes, (1990) replicated the CO_2 change over the last 100 kyrs of the Vostok ice core from DSDP Site 619 (Gulf of Mexico~~); Figure 1,6~~) and ~~(~~Bae et al., (2015) are able to replicate the ice core data at a site in the Japan Sea, records from the Arabian Sea (Palmer et al., 2010), Angola Current (Andersen et al., 1999) and the equatorial Atlantic (Zhang et al., 2013) either fail to record ice core CO_2 or require additional corrections to do so (Figure 7). ~~. However,~~ It may also be that at some sites, such as at ~~a record from the~~ Equatorial Pacific Site ~~(~~MANOP site C~~;~~ (Figure 1, 7~~6~~)~~-~~ these records represent changing air-sea disequilibrum ~~also failed to replicate the pCO_2 changes observed in the ice core data over the last 255 kyrs, and instead was interpreted as recording changes in air-sea equilibrium, not atmospheric CO_2~~ (Jasper et al., 1994). ~~Smoothing and correction for estimated growth rates revealed the gross features of the ice core record (Stoll and Schrag, 2000), but still only recorded 30-35 % of the variance in the ice core data (Bereiter et al., 2015; Stoll and Schrag, 2000). These~~ T~~t~~wo of these studies interpreted their data using a different ε_p relationship than later work; when these data are recalculated using the more recent model the patterns remain unchanged (Figure 7~~6~~). What is more, in a global alkenone $\delta^{13}C$ calibration study (Pagani et al., 2002) aimed at replicating Holocene atmospheric conditions it was noted that low latitude (sub-tropical) sites perform poorly, consistent with our observations. Considering this

present study and previously published work, ~~3~~ 5 out of ~~4~~ 7 late Pleistocene alkenone $\delta^{13}C$ studies do not show the variations in pCO_2 evident from contemporaneous ice core records (Figure 2; Figure 7~~6~~).

Our Bayesian approach allows us to explore the $CO_{2(\varepsilon p\text{-}alk)}$ proxy, as it was mathematically expressed by Bidigare et al (1997) and subsequent authors, and test which~~what~~ variables may be responsible for causing the observed disagreements with the ice core and $CO_{2(\delta 11Bplank)}$ records given a largely invariant ε_p for the Pleistocene.~~.~~ Figure 8~~7~~ illustrates the prior distributions of the input variables (blue) and an example posterior for the alkenone sample at 150 kyr (red). As can be seen in this example, selecting only those simulations of $CO_{2(\varepsilon p\text{-}alk)}$ that overlap with the ice core CO_2 for this time interval shifts the distributions such that an agreement is found when b is lower than the prior, ε_f tends to be higher than the prior and SST and CO_2 disequilibrium are little different. Figure 9~~8~~ shows the posterior median and 95 % distribution of b, ε_f and SST for all the samples from the Pleistocene and Pliocene in time series. Patterns that emerge are illustrated in Figure 10~~9~~, where a negative relationship between pCO_2 and posterior ε_f and a positive relationship between pCO_2 and posterior b and SST is evident. For SST it should also be noted that for the Pleistocene the posterior correlates well with the prior, while for the Pliocene it is significantly elevated (Figure 10~~9~~), perhaps suggesting a role for incorrect SST in driving some of the lack of Pliocene to Pleistocene change in $CO_{2(\varepsilon p\text{-}alk)}$ observed (Figure 2). This SST change would however need to be substantial and go beyond the ±2 °C we include in our uncertainty propagation, and would also potentially influence $CO_{2(\delta 11Bplank)}$, further complicating this finding.

We recognize that the nature of the patterns we observe here is a function somewhat of the range used for each input term. The chosen ranges are however conservative, but realistic, assessments of the likely uncertainty associated with each term. For instance, b ± 40 encompasses the residual scatter around the relationship between b and $[PO_4]$ described by Pagani et al., (2005). In addition to pointing towards a potential underestimate of Pliocene SST with the $U^{K'}_{37}$~~U$^{K'}_{37}$~~ proxy at ODP 999, this Bayesian treatment supports the assertion that the current understanding of the $CO_{2(\varepsilon p\text{-}alk)}$ proxy is wanting and that the b term may not in fact capture the scaling of the relevent physiological parameters or those that are truly important. In particular, it appears that the physiological parameters packaged in the b-term, and potentially the degree of fractionation upon fixation, ε_f, are themselves a function of CO_2 or some parameter that correlates with CO_2 (e.g. temperature, nutrients, growth rate etc.).

As noted above mean lith size is significantly different for the Pliocene and Pleistocene. A comparison of our posterior b and lith size does reveal a good correlation between these variables (Figure 11; $r^2 = 0.52$, $p<<0.01$), though this is largely, but not exclusively, a function of the mean change across the Plio-Pleistocene. Importantly, the observed relationship between b and lith size is very different from that described in ~~(~~Henderiks and Pagani, (2007). Suggesting that if lith size is important, our understanding, at least as laid out in ~~(~~Henderiks and Pagani, (2007) is incorrect.

An alternative explanation however could be that the ~~invariant~~ parameterisation of physiological factors into the 'b' term-model ~~could be~~is simply flawed in general, or is at least lacking important components. The dominant species producing alkenones in this part of the Caribbean today~~, and likely since its first appearance 268 kyrs ago~~, is *Emiliania huxleyi* (Winter et al., 2002). *E. huxleyi* first appears 290 kyrs ago, but did not become the dominant Noelaerhabdaceae until ~82 Ka when it began to outcompete the closely related *Gephyrocapsa* spp. which in in turn took over from *Reticulofenestra* in the late Pliocene (Gradstein et al., 2012; Raffi et al., 2006)~~.~~. Both our ~~Pleistocene~~ alkenone record~~s~~ are therefore a composite of closely-related but distinct noelaerhabdaceaen species, with nether record dominated by *E. huxleyi*. We cannot rule out ~~-~~that there could be physiological differences between the extant *E. huxleyi* species and the alkenone producers for our record. However the Site 925 $CO_{2(\varepsilon p\text{-}alk)}$ record of the last glacial-interglacial cycle, which would been primarily sourced from *E. huxleyi* is similarly flat, suggesting that species specific biosynthesis differences are unlikely to be the whole story. The *Reticulofenestra-Gephyrocapsa-Emiliania* lineage has strong stratigraphic, morphological and genetic support, with *Emiliani* and *Gephyrocapsa* only recently genetically diverging (Bendif et al., 2016). Likely these taxa shared the same or similar ecologies. Recent experimental work has shown that this globally important species has evolved a carbon concentrating mechanism (CCM) to respond to limiting CO_2 by upregulating genes at low DIC to maintain carbon requirements (Bach et al., 2013). CCMs result in a breakdown of the relationship between ε_p and CO_2 as defined and calibrated by Bidigare et al., (1997). It has been thought that the increased expression of CCMs will cause ε_p values to decrease, due to the isotopic offset between $CO_{2(aq)}$ and HCO_3^- and decreased carbon leakage from the cell (Zhang et al., 2013), effectively exacerbating the expected trend towards lower ε_p values at lower pCO_2 and inconsistent with our observation of relatively stable ε_p values across G-IG cycles.

However, CCMs appear to modulate carbon flow across cellular compartments (e.g. cytosol, chloroplast and calcification vesicle), and could also yield elevated rather than lower ε_p due to the concentrating of CO_2 at the site of carbon fixation (Bolton and Stoll, 2013). Additionally, as temperature modulates resource allocation between biosynthesis and photosynthesis (Sett et al., 2014), CO_2 optima are species specific and vary with temperature which may explain why some sites in the region with different dominant haptophyte species are capable of recording G-IG changes, whilst others struggle. ~~as temperature modulates resource allocation between biosynthesis and photosynthesis (Sett et al., 2014)~~. Furthermore, it has been postulated that changes in carbonate chemistry affect the redox state inside *E. huxleyi* cells which subsequently causes a reorganization of carbon flux within and across cellular compartments (Rokitta et al., 2012). Such a re-distribution of inorganic carbon amongst different pathways also likely influences ε_p and is currently not mechanistically represented by Bidigare et al., (1997) and other models.

4. Conclusions

Our data show that the classical application of the alkenone pCO_2 proxy fails to capture glacial-interglacial changes observed in the ice cores. With increased confidence in $CO_{2(\delta 11Bplank)}$ supplied by that proxy's ability to capture Pleistocene pCO_2 variability, our data also suggest that the discrepancy between $CO_{2(\delta 11Bplank)}$ and $CO_{2(\varepsilon p\text{-}alk)}$ in the Pliocene may also be due to problems with $CO_{2(\varepsilon p\text{-}alk)}$. Emerging insights into coccolithophore CO_2 allocation pathways and their sensitivity to CO_2 and temperature, in conjunction with our inter-proxy comparisons, indicate that the long-standing $CO_{2(\varepsilon p\text{-}alk)}$ proxy requires major revision and recalibration. If CCMs are preferentially more important for the alkenone palaeobarometer than growth rate, the muted alkenone palaeobarometer response may be limited to the low CO_2 world of the Plio-Pleistocene and particularly in tropical waters where $CO_{2[aq]}$ is especially low. By extension, this proxy (and interpretations based on it) likely retains utility at the higher CO_2 levels typical of the early Cenozoic (and at high latitudes where $CO_{2[aq]}$ is high) where active carbon uptake is less likely (Zhang et al., 2013). This is especially true if haptophyte CCMs only evolved in the late Miocene as a response to declining CO_2 levels (Bolton and Stoll, 2013). Regardless, the discrepancy between $CO_{2(\varepsilon p\text{-}alk)}$ and ice core CO_2 records indicates that alkenone isotopes in several locations do not faithfully record atmospheric CO_2 at relatively low, Plio-Pleistocene-like CO_2 levels. Furthermore, the muted response of $CO_{2(\varepsilon p\text{-}alk)}$ to $[CO_{2(aq)}]$ at lower concentrations calls into

question the underlying basis of the high climate sensitivities previously reconstructed using this method in the Plio-Pleistocene (Pagani et al., 2009). This, coupled with further evidence of the fidelity of $CO_{2(\delta 11Bplank)}$ at Site 999 suggests that the climate sensitivities derived from $CO_{2(\delta 11Bplank)}$ (which are consistent with climate models used both in palaeoclimate and future climate projections) are more accurate (Martínez-Botí et al., 2015~~a~~).

Author contributions

MPSB and GLF conceived the study [conceptualization], MPSB, TBC and GLF designed the methodology, carried out data collection and analysed the data [formal analysis, investigation, methodology]. PRB, SJG, HP and AM performed data collection, PFS finalised the age model [investigation]. MPSB wrote the manuscript and prepared figures [Visualisation, Writing – original draft]. RDP (PI) and GLF and DNS (CoIs) supervised the project and acquired funding [Funding acquisition & Supervision]. All authors contributed to interpretation, writing and reviewing the manuscript [Writing – review & editing].

Acknowledgements

This study used samples provided by the International Ocean Discovery Program (IODP). We thank Alex Hull and Gemma Bowler for laboratory work, Lisa Schönborn and Günter Meyer for technical assistance, Alison Kuhl and Ian Bull for research support, and Andy Milton at the University of Southampton for maintaining some of the mass spectrometers used in this study. This study was funded by NERC grant NE/H006273/1 to RDP, DNS and GLF (which supported MPSB). We also acknowledge the ERC Award T-GRES and a Royal Society Wolfson Research Merit Award to RDP. GLF is also supported by a Royal Society Wolfson Research Merit Award. We thank Kirsty Edgar for comments on an early draft of the manuscript, the two anonymous reviewers of this submission, and reviewers through various rounds of review whose comments greatly improved the manuscript. We are grateful to Thomas Bauska for encouraging us to do better at referencing the ice core data, and John Jasper for discussion of the early days of the alkenone palaeobarometer.

References

Ahn, J. and Brook, E. J.: Siple Dome ice reveals two modes of millennial CO2 change during the last ice age, Nat. Commun., 5, 3723 [online] Available from: http://dx.doi.org/10.1038/ncomms4723, 2014.

Ahn, J., Brook, E. J., Mitchell, L., Rosen, J., McConnell, J. R., Taylor, K., Etheridge, D. and Rubino, M.: Atmospheric CO2 over the last 1000 years: A high-resolution record from the West Antarctic Ice Sheet (WAIS) Divide ice core, Global Biogeochem. Cycles, 26(2), n/a-n/a, doi:10.1029/2011GB004247, 2012.

Anagnostou, E., John, E. H., Edgar, K. M., Foster, G. L., Ridgwell, A., Inglis, G. N., Pancost, R. D., Lunt, D. J. and Pearson,

P. N.: Changing atmospheric CO2 concentration was the primary driver of early Cenozoic climate, Nature, 533(7603), 380–384, doi:10.1038/nature17423, 2016.

Andersen, N., Miiller, P. J., Kirsf, G. and Schneider, R. R.: Alkenone delta-13C as a proxy for past pCO2 in surface waters: Results from the Late Quarternary Angola Current, 1999.

Bach, L. T., Mackinder, L. C. M., Schulz, K. G., Wheeler, G., Schroeder, D. C., Brownlee, C. and Riebesell, U.: Dissecting the impact of CO2 and pH on the mechanisms of photosynthesis and calcification in the coccolithophore Emiliania huxleyi., New Phytol., 199(1), 121–34, doi:10.1111/nph.12225, 2013.

Badger, M. P. S., Schmidt, D. N., Mackensen, A. and Pancost, R. D.: High-resolution alkenone palaeobarometry indicates relatively stable pCO(2) during the Pliocene (3.3-2.8 Ma)., Philos. Trans. A. Math. Phys. Eng. Sci., 371, 20130094, doi:10.1098/rsta.2013.0094, 2013a.

Badger, M. P. S. S., Lear, C. H., Pancost, R. D., Foster, G. L., Bailey, T. R., Leng, M. J. and Abels, H. a.: CO2 drawdown following the middle Miocene expansion of the Antarctic Ice Sheet, Paleoceanography, 28(1), 42–53, doi:10.1002/palo.20015, 2013b.

Bae, S. W., Lee, K. E. and Kim, K.: Use of carbon isotopic composition of alkenone as a CO2 proxy in the East Sea/Japan Sea, Cont. Shelf Res., 107, 24–32, doi:10.1016/j.csr.2015.07.010, 2015.

Bartoli, G., Hönisch, B. and Zeebe, R. E.: Atmospheric CO 2 decline during the Pliocene intensification of Northern Hemisphere glaciations, Paleoceanography, 26(4), n/a--n/a, doi:10.1029/2010PA002055, 2011.

Bendif, E. M., Probert, I., Díaz-Rosas, F., Thomas, D., van den Engh, G., Young, J. R. and von Dassow, P.: Recent reticulate evolution in the ecologically dominant lineage of coccolithophores, Front. Microbiol., 7(MAY), doi:10.3389/fmicb.2016.00784, 2016.

Bereiter, B., Lüthi, D., Siegrist, M., Schüpbach, S., Stocker, T. F. and Fischer, H.: Mode change of millennial CO2 variability during the last glacial cycle associated with a bipolar marine carbon seesaw, Proc. Natl. Acad. Sci., 109(25), 9755–9760, doi:10.1073/pnas.1204069109, 2012.

Bereiter, B., Eggleston, S., Schmitt, J., Nehrbass-Ahles, C., Stocker, T. F., Fischer, H., Kipfstuhl, S. and Chappellaz, J.: Revision of the EPICA Dome C CO 2 record from 800 to 600 kyr before present, Geophys. Res. Lett., 42(2), 542–549, doi:10.1002/2014GL061957, 2015.

Bidigare, R., Fluegge, A., Freeman, K. H., Hanson, K., Hayes, J. M., Hollander, D., Jasper, J. P., King, L. L., Laws, E., Milder, J., Millero, F. J., Pancost, R., Popp, B. N., Steinberg, P. and Wakeham, S. G.: Consistent fractionation of 13C in nature and in the laboratory: Growth-rate effects in some haptophyte algae, Global Biogeochem. Cycles, 11(2), 279–292 [online] Available from: http://onlinelibrary.wiley.com/doi/10.1029/96GB03939/full (Accessed 12 January 2015), 1997.

Bolton, C. T. and Stoll, H. M.: Late Miocene threshold response of marine algae to carbon dioxide limitation., Nature,

500(7464), 558–62, doi:10.1038/nature12448, 2013.

Chalk, T. B., Hain, M. P., Foster, G. L., Rohling, E. J., Sexton, P. F., Badger, M. P. S., Cherry, S. G., Hasenfratz, A. P., Haug, G. H., Jaccard, S. L., Martínez-García, A., Pälike, H., Pancost, R. D. and Wilson, P. A.: Causes of ice age intensification across the Mid-Pleistocene Transition, Proc. Natl. Acad. Sci., 201702143, doi:10.1073/pnas.1702143114, 2017.

Davis, C. V. V., Badger, M. P. S. P. S., Bown, P. R. R. and Schmidt, D. N. N.: The response of calcifying plankton to climate change in the Pliocene, Biogeosciences, 10(9), 6131–6139, doi:10.5194/bg-10-6131-2013, 2013.

Delaney, M. L. and Boyle, E. A.: Li, Sr, Mg, and Na in foraminiferal calcite shells from laboratory culture , sediment traps, and sediment cores, Geochim. Cosmochim. Acta, 49(October 1983), 1327–1341, 1985.

Dickson, A. G.: Thermodynamics of the dissociation of boric acid in synthetic seawater from 273.15 to 318.15 K, Deep Sea Res. Part A. Oceanogr. Res. Pap., 37(5), 755–766, doi:10.1016/0198-0149(90)90004-F, 1990.

Evans, D. and Müller, W.: Deep time foraminifera Mg/Ca paleothermometry: Nonlinear correction for secular change in seawater Mg/Ca, Paleoceanography, 27(4), n/a--n/a, doi:10.1029/2012PA002315, 2012.

Foster, G. L.: Seawater pH, pCO2 and [CO2−3] variations in the Caribbean Sea over the last 130 kyr: A boron isotope and B/Ca study of planktic foraminifera, Earth Planet. Sci. Lett., 271(1–4), 254–266, doi:10.1016/j.epsl.2008.04.015, 2008.

Foster, G. L. and Sexton, P. F.: Enhanced carbon dioxide outgassing from the eastern equatorial Atlantic during the last glacial, Geology, 42(11), 1003–1006, doi:10.1130/G35806.1, 2014.

Foster, G. L., Hönisch, B., Paris, G., Dwyer, G. S., Rae, J. W. B. B., Elliott, T., Gaillardet, J., Hemming, N. G., Louvat, P. and Vengosh, A.: Interlaboratory comparison of boron isotope analyses of boric acid, seawater and marine CaCO3 by MC-ICPMS and NTIMS, Chem. Geol., 358, 1–14, doi:10.1016/j.chemgeo.2013.08.027, 2013.

Foster, G. L., Royer, D. L. and Lunt, D. J.: Future climate forcing potentially without precedent in the last 420 million years, Nat. Commun., 8, 14845, doi:10.1038/ncomms14845, 2017.

Gattuso, J.-P., Epitalalon, J.-M. and Lavigne, H.: Seacarb: Seawater Carbonate Chemistry. R package version 3.0.8, 2015.

Gibbs, S. J., Poulton, A. J., Bown, P. R., Daniels, C. J., Hopkins, J., Young, J. R., Jones, H. L., Thiemann, G. J., O'Dea, S. A. and Newsam, C.: Species-specific growth response of coccolithophores to Palaeocene–Eocene environmental change, Nat. Geosci., 6(3), 218–222, doi:10.1038/ngeo1719, 2013.

Gradstein, F., Ogg, J., Schmitz, M. and Ogg, G.: The Geologic Time Scale 2012, 1st ed., edited by F. Gradstein, J. Ogg, M. Schmitz, and G. Ogg, Elsevier., 2012.

Hemming, N. G. and Hanson, G. N.: Boron isotopic composition and concentration in modern marine carbonates, Geochim. Cosmochim. Acta, 56(1), 537–543, doi:10.1016/0016-7037(92)90151-8, 1992.

Henderiks, J.: Coccolithophore size rules — Reconstructing ancient cell geometry and cellular calcite quota from fossil

coccoliths, Mar. Micropaleontol., 67(1–2), 143–154, doi:10.1016/j.marmicro.2008.01.005, 2008.

Henderiks, J. and Pagani, M.: Refining ancient carbon dioxide estimates: Significance of coccolithophore cell size for alkenone-based p CO 2 records, Paleoceanography, 22(3), n/a-n/a, doi:10.1029/2006PA001399, 2007.

Henehan, M. J., Rae, J. W. B. B., Foster, G. L., Erez, J., Prentice, K. C., Kucera, M., Bostock, H. C., Martínez-Botí, M. A., Milton, J. A., Wilson, P. A., Marshall, B. J. and Elliott, T.: Calibration of the boron isotope proxy in the planktonic foraminifera Globigerinoides ruber for use in palaeo-CO2 reconstruction, Earth Planet. Sci. Lett., 364, 111–122, doi:10.1016/j.epsl.2012.12.029, 2013.

Hönisch, B. and Hemming, N. G.: Surface ocean pH response to variations in pCO2 through two full glacial cycles, Earth Planet. Sci. Lett., 236(1–2), 305–314, doi:10.1016/j.epsl.2005.04.027, 2005.

Jasper, J. and Hayes, J.: A carbon isotope record of CO2 levels during the late Quaternary, Nature, 347, 462–464 [online] Available from: http://www.nature.com/nature/journal/v347/n6292/abs/347462a0.html (Accessed 12 January 2015), 1990.

Jasper, J., Hayes, J., Mix, A. and Prahl, F.: Photosynthetic fractionation of 13C and concentrations of dissolved CO2 in the central equatorial Pacific during the last 255,000 years, Paleoceanography, 9(6), 781–798 [online] Available from: http://onlinelibrary.wiley.com/doi/10.1029/94PA02116/full (Accessed 12 January 2015), 1994.

Klochko, K., Kaufman, A. J., Yao, W., Byrne, R. H. and Tossell, J. A.: Experimental measurement of boron isotope fractionation in seawater, Earth Planet. Sci. Lett., 248(1–2), 276–285, doi:10.1016/j.epsl.2006.05.034, 2006.

Lacis, A. A., Schmidt, G. A., Rind, D. and Ruedy, R. A.: Atmospheric CO2: Principal Control Knob Governing Earth's Temperature, Science (80-.)., 330(6002), 356–359, doi:10.1126/science.1190653, 2010.

Laws, E. a., Bidigare, R. R. and Popp, B. N.: Effect of growth rate and CO2 concentration on carbon isotopic fractionation by the marine diatom Phaeodactylum tricornutum, Limnol. Oceanogr., 42(7), 1552–1560, doi:10.4319/lo.1997.42.7.1552, 1997.

Lisiecki, L. E. and Raymo, M. E.: A Pliocene-Pleistocene stack of 57 globally distributed benthic δ 18 O records, Paleoceanography, 20(1), n/a-n/a, doi:10.1029/2004PA001071, 2005.

MacFarling Meure, C., Etheridge, D., Trudinger, C., Steele, P., Langenfelds, R., van Ommen, T., Smith, A. and Elkins, J.: Law Dome CO2, CH4 and N2O ice core records extended to 2000 years BP, Geophys. Res. Lett., 33(14), L14810, doi:10.1029/2006gl026152, 2006.

Marcott, S. A., Bauska, T. K., Buizert, C., Steig, E. J., Rosen, J. L., Cuffey, K. M., Fudge, T. J., Severinghaus, J. P., Ahn, J., Kalk, M. L., McConnell, J. R., Sowers, T., Taylor, K. C., White, J. W. C. and Brook, E. J.: Centennial-scale changes in the global carbon cycle during the last deglaciation, Nature, 514(7524), 616–619 [online] Available from: http://dx.doi.org/10.1038/nature13799, 2014.

Martínez-Botí, M. A., Foster, G. L., Chalk, T. B., Rohling, E. J., Sexton, P. F., Lunt, D. J., Pancost, R. D., Badger, M. P. S. S.

and Schmidt, D. N.: Plio-Pleistocene climate sensitivity evaluated using high-resolution CO2 records, Nature, 518(7537), 49–54, doi:10.1038/nature14145, 2015.

Monnin, E., Indermuhle, A., Dallenbach, A., Fluckiger, J., Stauffer, B., Stocker, T. F., Raynaud, D. and Barnola, J. M.: Atmospheric CO2 concentrations over the last glacial termination, Science (80-.)., 291(5501), 112–114, doi:10.1126/science.291.5501.112, 2001.

Monnin, E., Steig, E. J., Siegenthaler, U., Kawamura, K., Schwander, J., Stauffer, B., Stocker, T. F., Morse, D. L., Barnola, J.-M., Bellier, B., Raynaud, D. and Fischer, H.: Evidence for substantial accumulation rate variability in Antarctica during the Holocene, through synchronization of CO2 in the Taylor Dome, Dome C and DML ice cores, Earth Planet. Sci. Lett., 224(1–2), 45–54, doi:10.1016/j.epsl.2004.05.007, 2004.

Müller, P., Kirst, G., Ruhland, G., von Storch, I. and Rosell-Melé, A.: Calibration of the alkenone paleotemperature index U 37 K′ based on core-tops from the eastern South Atlantic and the global ocean (60 N - 60 S), Geochim. Cosmochim. Acta, 62(10), 1757–1772 [online] Available from: http://www.sciencedirect.com/science/article/pii/S0016703798000970 (Accessed 13 January 2015), 1998.

Pagani, M., Freeman, K. H., Ohkouchi, N. and Caldeira, K.: Comparison of water column [CO 2aq] with sedimentary alkenone-based estimates: A test of the alkenone-CO 2 proxy, Paleoceanography, 17(4), 21-1-21–12, doi:10.1029/2002PA000756, 2002.

Pagani, M., Zachos, J. C., Freeman, K. H., Tipple, B. and Bohaty, S.: Marked decline in atmospheric carbon dioxide concentrations during the Paleogene., Science, 309(5734), 600–603, doi:10.1126/science.1110063, 2005.

Pagani, M., Liu, Z., LaRiviere, J. and Ravelo, A. C.: High Earth-system climate sensitivity determined from Pliocene carbon dioxide concentrations, Nat. Geosci., 3(1), 27–30, doi:10.1038/ngeo724, 2009.

Pagani, M., Huber, M., Liu, Z., Bohaty, S. M., Henderiks, J., Sijp, W., Krishnan, S. and DeConto, R. M.: The role of carbon dioxide during the onset of Antarctic glaciation., Science, 334(6060), 1261–4, doi:10.1126/science.1203909, 2011.

Paillard, D., Labeyrie, L. and Yiou, P.: Macintosh Program performs time-series analysis, Eos, Trans. Am. Geophys. Union, 77(39), 379–379, doi:10.1029/96EO00259, 1996.

PALAEOSENS: Making sense of palaeoclimate sensitivity., Nature, 491(7426), 683–91, doi:10.1038/nature11574, 2012.

Palmer, M. R. R., Brummer, G. J. J., Cooper, M. J. J., Elderfield, H., Greaves, M. J. J., Reichart, G. J. J., Schouten, S. and Yu, J. M. M.: Multi-proxy reconstruction of surface water pCO2 in the northern Arabian Sea since 29ka, Earth Planet. Sci. Lett., 295(1–2), 49–57, doi:10.1016/j.epsl.2010.03.023, 2010.

Pearson, P. N., Foster, G. L. and Wade, B. S.: Atmospheric carbon dioxide through the Eocene-Oligocene climate transition., Nature, 461(7267), 1110–1113, doi:10.1038/nature08447, 2009.

Petit, J. R., Jouzel, J., Raynaud, D., Barkov, N. I., Barnola, J.-M., Basile, I., Bender, M., Chappellaz, J., Davis, M., Delaygue, G., Delmotte, M., Kotlyakov, V. M., Legrand, M., Lipenkov, V. Y., Lorius, C., Pepin, K., Ritz, C., Saltzman, E. and Stievenard, M.: Climate and atmospheric history of the past 420,000 years from the Vostok ice core, Antarctica, Nature, 399, 429–436 [online] Available from: http://www.nature.com/nature/journal/v399/n6735/abs/399429a0.html (Accessed 12 January 2015), 1999.

Popp, B., Laws, E., Bidigare, R., Dore, J., Hanson, K. and Wakeham, S. G.: Effect of phytoplankton cell geometry on carbon isotopic fractionation, Geochim. Cosmochim. Acta, 62(1), 67–77 [online] Available from: http://www.sciencedirect.com/science/article/pii/S0016703797003335 (Accessed 12 January 2015), 1998.

Rae, J. W. B. B., Foster, G. L., Schmidt, D. N. and Elliott, T.: Boron isotopes and B/Ca in benthic foraminifera: Proxies for the deep ocean carbonate system, Earth Planet. Sci. Lett., 302(3–4), 403–413, doi:10.1016/j.epsl.2010.12.034, 2011.

Raffi, I., Backman, J., Fornaciari, E., Pälike, H., Rio, D., Lourens, L. and Hilgen, F.: A review of calcareous nannofossil astrobiochronology encompassing the past 25 million years☆, Quat. Sci. Rev., 25(23–24), 3113–3137, doi:10.1016/j.quascirev.2006.07.007, 2006.

Rokitta, S. D., John, U. and Rost, B.: Ocean Acidification Affects Redox-Balance and Ion-Homeostasis in the Life-Cycle Stages of Emiliania huxleyi, edited by S. Dupont, PLoS One, 7(12), e52212, doi:10.1371/journal.pone.0052212, 2012.

Rubino, M., Etheridge, D. M., Trudinger, C. M., Allison, C. E., Battle, M. O., Langenfelds, R. L., Steele, L. P., Curran, M., Bender, M., White, J. W. C., Jenk, T. M., Blunier, T. and Francey, R. J.: A revised 1000 year atmospheric δ13C-CO2 record from Law Dome and South Pole, Antarctica, J. Geophys. Res. Atmos., 118(15), 8482–8499, doi:10.1002/jgrd.50668, 2013.

Sanyal, A. and Hemming, N.: Oceanic pH control on the boron isotopic composition of foraminifera: evidence from culture experiments, Paleoceanography, 11(5), 513–517 [online] Available from: http://onlinelibrary.wiley.com/doi/10.1029/96PA01858/full (Accessed 12 January 2015), 1996.

Sanyal, A., Hemming, N., Hanson, G. and Broecker, W.: Evidence for a higher pH in the glacial ocean from boron isotopes in foraminifera, Nature, 373, 234–236 [online] Available from: http://www.pmc.ucsc.edu/~apaytan/290A_Winter2014/pdfs/B isotopes Jn 24-1.pdf (Accessed 12 January 2015), 1995.

Schmidt, M. W., Vautravers, M. J. and Spero, H. J.: Western Caribbean sea surface temperatures during the late Quaternary, Geochemistry, Geophys. Geosystems, 7(2), n/a-n/a, doi:10.1029/2005GC000957, 2006.

Schneider, R., Schmitt, J., Köhler, P., Joos, F. and Fischer, H.: A reconstruction of atmospheric carbon dioxide and its stable carbon isotopic composition from the penultimate glacial maximum to the last glacial inception, Clim. Past, 9(6), 2507–2523, 2013.

Seki, O., Foster, G. L., Schmidt, D. N., Mackensen, A., Kawamura, K. and Pancost, R. D.: Alkenone and boron-based Pliocene pCO2 records, Earth Planet. Sci. Lett., 292(1–2), 201–211, doi:10.1016/j.epsl.2010.01.037, 2010.

Sett, S., Bach, L. T., Schulz, K. G., Koch-Klavsen, S., Lebrato, M. and Riebesell, U.: Temperature modulates coccolithophorid sensitivity of growth, photosynthesis and calcification to increasing seawater pCO_2., PLoS One, 9(2), e88308, doi:10.1371/journal.pone.0088308, 2014.

Sheward, R. M., Poulton, A. J., Gibbs, S. J., Daniels, C. J. and Bown, P. R.: Physiology regulates the relationship between coccosphere geometry and growth phase in coccolithophores, Biogeosciences, 14(6), 1493–1509, doi:10.5194/bg-14-1493-2017, 2017.

Sosdian, S. M., Greenop, R., Hain, M. P., Foster, G. L., Pearson, P. N. and Lear, C. H.: Constraining the evolution of Neogene ocean carbonate chemistry using the boron isotope pH proxy, Earth Planet. Sci. Lett., 498, 362–376, doi:10.1016/J.EPSL.2018.06.017, 2018.

Super, J. R., Thomas, E., Pagani, M., Huber, M., Brien, C. O. and Hull, P. M.: North Atlantic temperature and pCO2 coupling in the early-middle Miocene, Geology, 46(6), 519–522, doi:https://doi.org/10.1130/G40228.1, 2018.

Takahashi, T., Sutherland, S. C., Wanninkhof, R., Sweeney, C., Feely, R. a., Chipman, D. W., Hales, B., Friederich, G., Chavez, F., Sabine, C., Watson, A., Bakker, D. C. E. E., Schuster, U., Metzl, N., Yoshikawa-Inoue, H., Ishii, M., Midorikawa, T., Nojiri, Y., Körtzinger, A., Steinhoff, T., Hoppema, M., Olafsson, J., Arnarson, T. S., Tilbrook, B., Johannessen, T., Olsen, A., Bellerby, R., Wong, C. S. S., Delille, B., Bates, N. R. R. and de Baar, H. J. W. W.: Climatological mean and decadal change in surface ocean pCO2, and net sea–air CO2 flux over the global oceans, Deep Sea Res. Part II Top. Stud. Oceanogr., 56(8–10), 554–577, doi:10.1016/j.dsr2.2008.12.009, 2009.

Team, R. C.: R: A language and environment for statistical computing, 2015.

Trumbo, S. K.: Marine Export Productivity and the Demise of the Central American Seaway, UC San Diego. [online] Available from: http://www.escholarship.org/uc/item/83f2w736, 2015.

Winter, A., Rost, B., Hilbrecht, H. and Elbrächter, M.: Vertical and horizontal distribution of coccolithophores in the Caribbean Sea, Geo-Marine Lett., 22(3), 150–161, doi:10.1007/s00367-002-0108-8, 2002.

YOUNG, J.: Size variation of Neogene Reticulofenestra coccoliths from Indian Ocean DSDP Cores, J. Micropalaeontology, 9(1), 71–85, doi:10.1144/jm.9.1.71, 1990.

Zhang, Y. G., Pagani, M., Liu, Z., Bohaty, S. M. and Deconto, R.: A 40-million-year history of atmospheric CO(2)., Philos. Trans. A. Math. Phys. Eng. Sci., 371(2001), 20130096, doi:10.1098/rsta.2013.0096, 2013.

Tables

Table 1: Sources of ice core data used throughout as compiled by (Bereiter et al., (2015)

Age interval (Kyr BP)	Ice core location	Reference
-0.051 – 1.8	Law Dome	Rubino et al., (2013)
1.8 – 2	Law Dome	MacFarling Meure et al., (2006)
2 – 11	Dome C	Monnin et al., 2001, (2004)
11 – 22	WAIS	Marcott et al., (2014)
22 – 40	Siple Dome	Ahn and Brook, (2014)
40 – 60	TALDICE	Bereiter et al., (2012)
60 – 115	EDML	Bereiter et al., (2012)
105 – 155	Dome C Sublimation	Schneider et al., (2013)
155 – 393	Vostok	Petit et al., (1999)

Figures

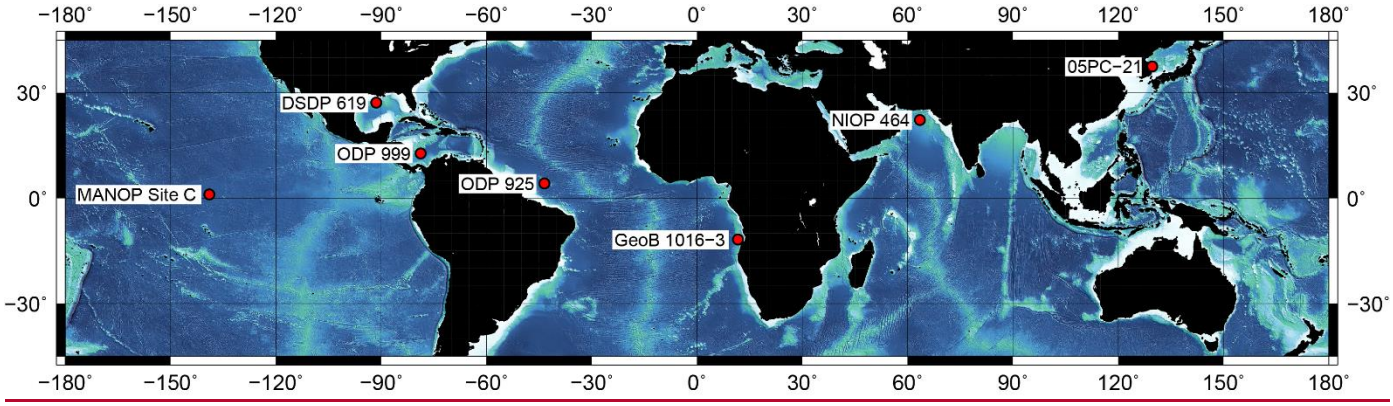

Figure 1 Site map. Locations of sites discussed the text.

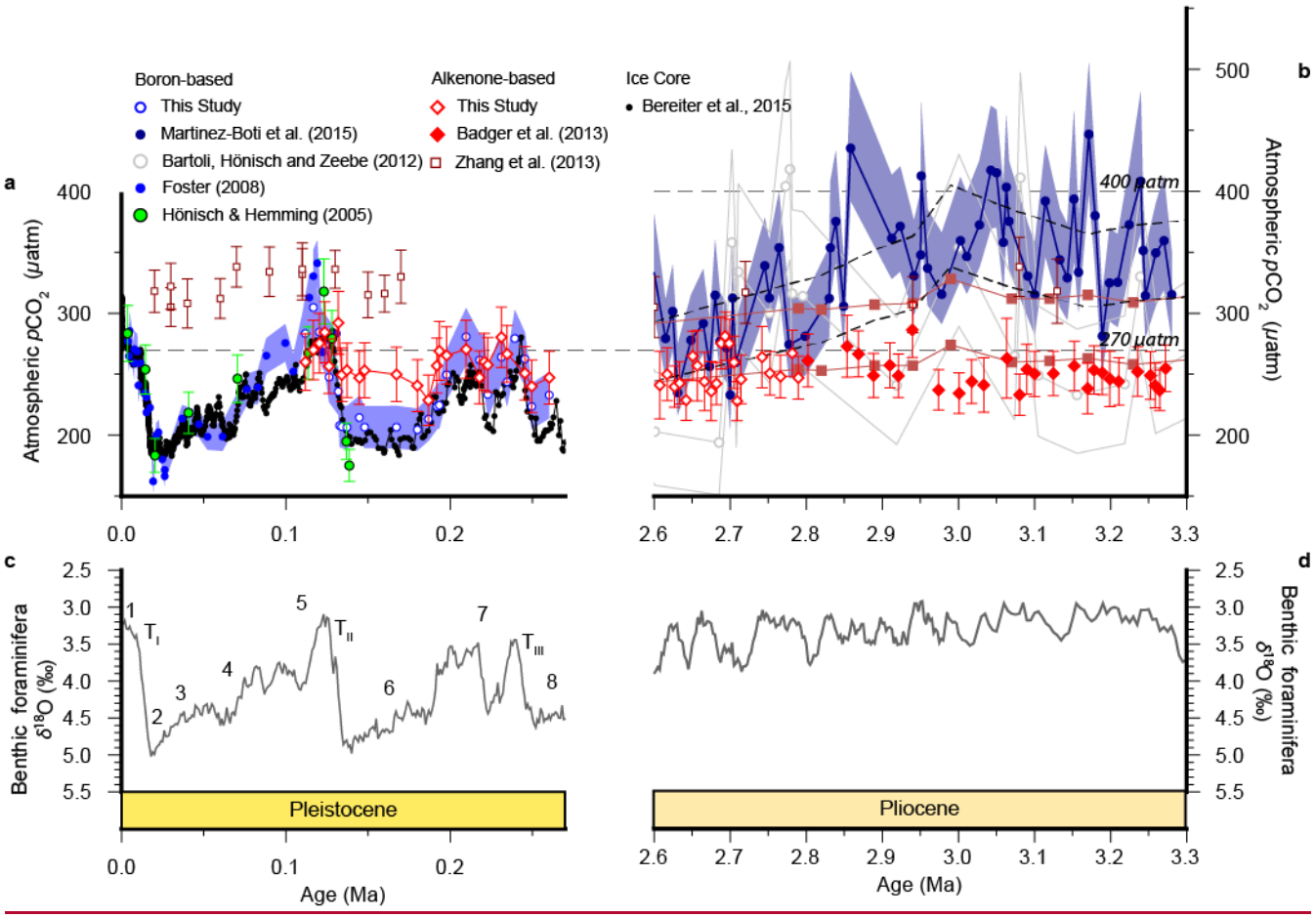

Figure 2 Atmospheric CO_2 reconstructions through the Plio-Pleistocene. a: Published boron isotope $CO_{2(\delta 11B plank)}$ records from ODP Site 999 (open blue circles; (Chalk et al., 2017)**, bright blue filled circles; (Foster, 2008 recalculated as described in the text), grey open circles** (Bartoli et al., 2011)**, dark blue filled circles** (Martínez-Botí et al., 2015)**) and DSDP Site 668 (green filled circles** (Hönisch and Hemming, 2005)**); b: published $CO_{2(\varepsilon p\text{-}alk)}$ records from ODP Site 925 (maroon open squares** (Zhang et al., 2013)**) and ODP Site 999 (red filled diamonds**(Badger et al., 2013b) **and ice core records (black filled squares** (Bereiter et al., 2015 and Table 1~~; Petit et al., 1999~~)**), as well as our new alkenone isotope records from ODP Site 999 (red open diamonds). The lith-size corrected (black dashed envelope) and uncorrected (red solid envelope) of Seki et al.,** (Seki et al., 2010) **are also shown. All records are shown with 1σ uncertainties as described elsewhere. c: benthic foraminiferal stable oxygen isotope stack** (Lisiecki and Raymo, 2005) **with Marine Isotope Stages (MIS; numerals) and Terminations (T) indicated.**

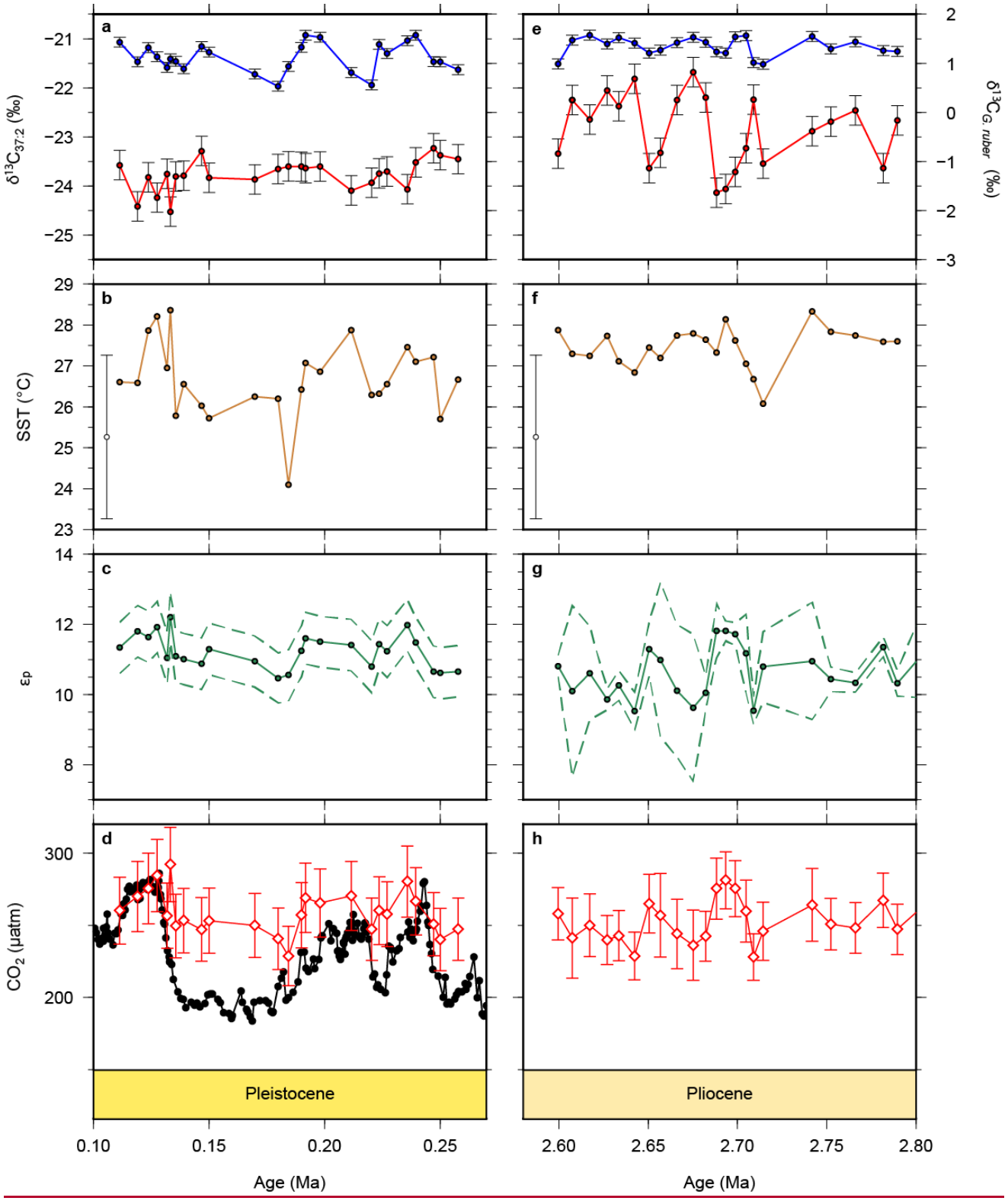
a
b
c
d
e
f
g
h
$\delta^{13}C_{37:2}$ (‰)
SST (°C)
ε_p
CO_2 (µatm)
$\delta^{13}C_{G.\ ruber}$ (‰)
Pleistocene
Pliocene
Age (Ma)
Age (Ma)

Figure 3 New and recalculated date for $CO_{2(\varepsilon p\text{-}alk)}$ for the Pleistocene and Pliocene from ODP Site 999. Alkenone $\delta^{13}C$ values are shown as red circles for the Pleistocene (a) and Pliocene (b) with *G. ruber* $\delta^{13}C$ from the same samples shown in blue. Alkenone unsaturation-derived SST is shown for the Pleistocene (b) and Pliocene (f). The Pliocene SST data has been previously published as Davis et al., 2013 and is from the same samples as our alkenone $\delta^{13}C$ values. Calculated ε_p data for the Pleistocene (c) and Pliocene (g) and atmospheric pCO_2 from $CO_{2(\varepsilon p\text{-}alk)}$ for the Pleistocene (d) and Pliocene (h) (red diamonds). Ice core pCO_2 data is shown for the Pleistocene (black circles) for comparison (Bereiter et al., 2015 and Table 1)**.**

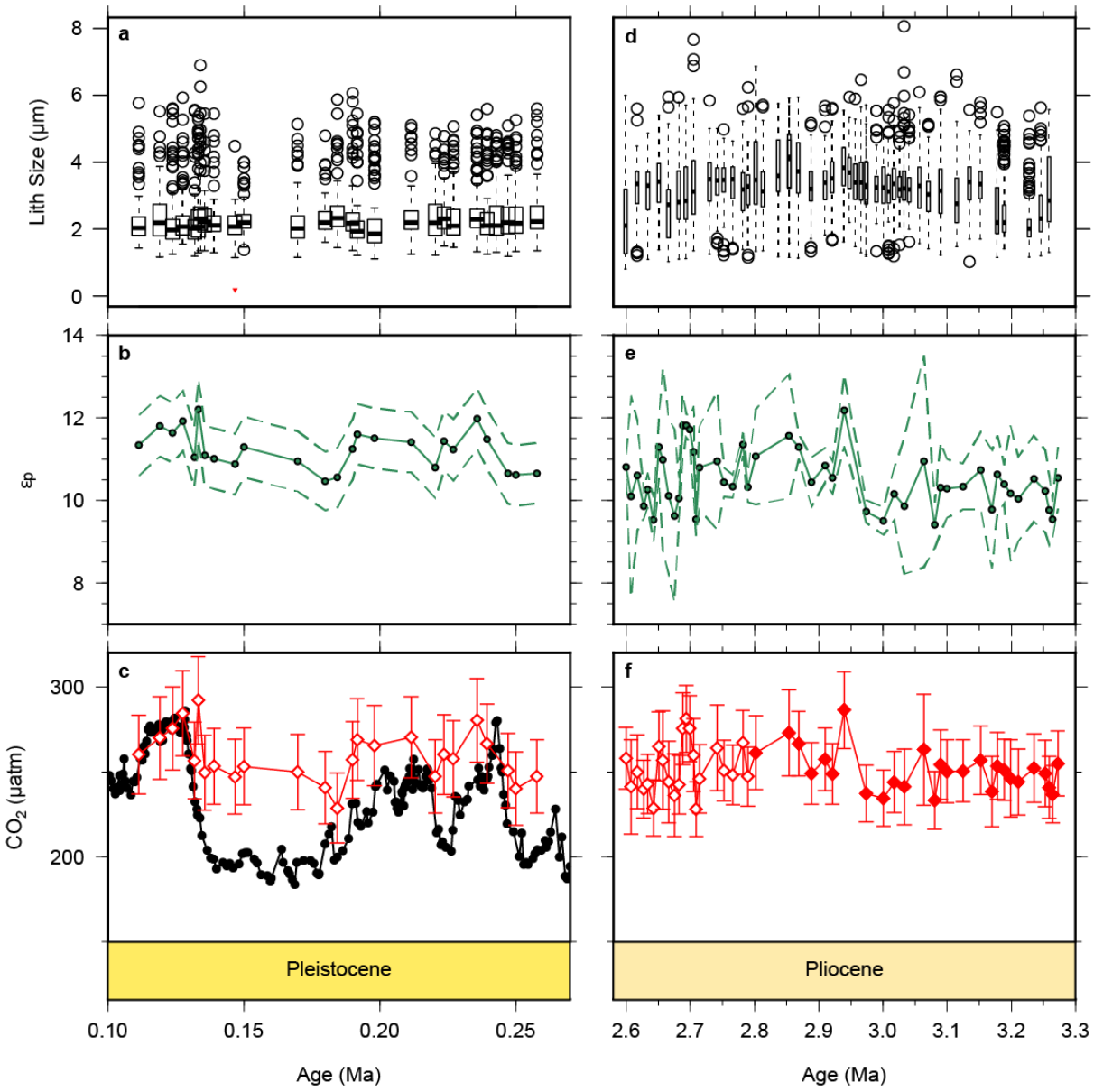

Figure 4 Lith Size data for samples used for CO_2 calculations. Pleistocene lith size (a~~b~~) are from this study, whilst Pliocene (b) values were published previously (Davis et al., 2013) **but are from the same samples as our CO_2 estimates. Pleistocene ε_p (b) are from this study, whilst the Pliocene data is from this study (2.6-2.8 Mar) and for** Badger et al., (2013b) **(2.8-3.3 Ma). The lower panels show $CO_{2(\varepsilon p\text{-}alk)}$ for the Plesistocene (c) and Pliocene (f) as red diamonds. The filled diamonds in (f) are** (Badger et al., 2013a)**. The Pleistocene ice core data** (Bereiter et al., 2015 and Table 1) **are shown for comparison in (c). The drop in lith size from the Pliocene to Pleistocene is similar to what has been documented previously** (YOUNG, 1990)**. Outliers in a and d were calculated following the 1.5 rule in R (R Core Team, 2015).**

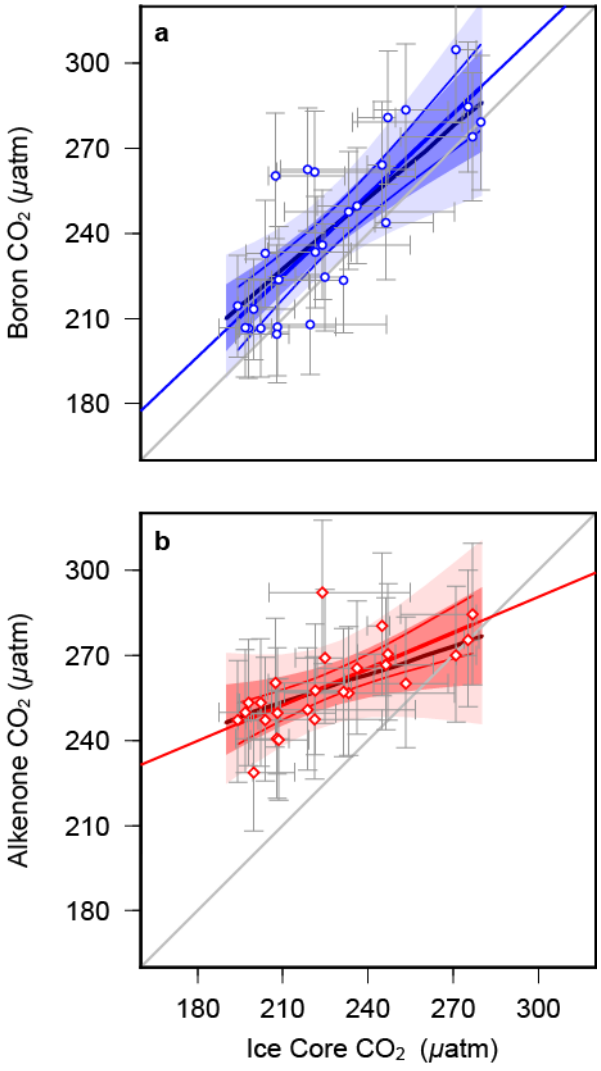
a
b
Boron CO_2 (μatm)
Alkenone CO_2 (μatm)
Ice Core CO_2 (μatm)
180
210
240
270
300

Figure 5 Regression analyses of proxy-based pCO_2 with ice core data a; $CO_{2(\delta 11Bplank)}$ (Chalk et al., 2017) **and b; $CO_{2(\varepsilon p\text{-}alk)}$ vs ice core data** (Bereiter et al., 2015 and Table 1) **for MIS5-8, interpolated in the age domain. Regression lines (in red/blue) are linear fits with 68 and 95 % confidence intervals, calculated by bootstrapping the uncertainties in proxy pCO_2 (Monte Carlo method described in methods). Uncertainty in the ice core values are by estimated by applying a 3000 uncertainty in the age model during interpolation. Uncertainty envelopes considering data points alone (no bootstrap) are solid lines, with pmax regressions in the thicker, darker colours. A 1:1 line is shown in grey for comparison. Statistical calculations were performed in R (R Core Team, 2015).**

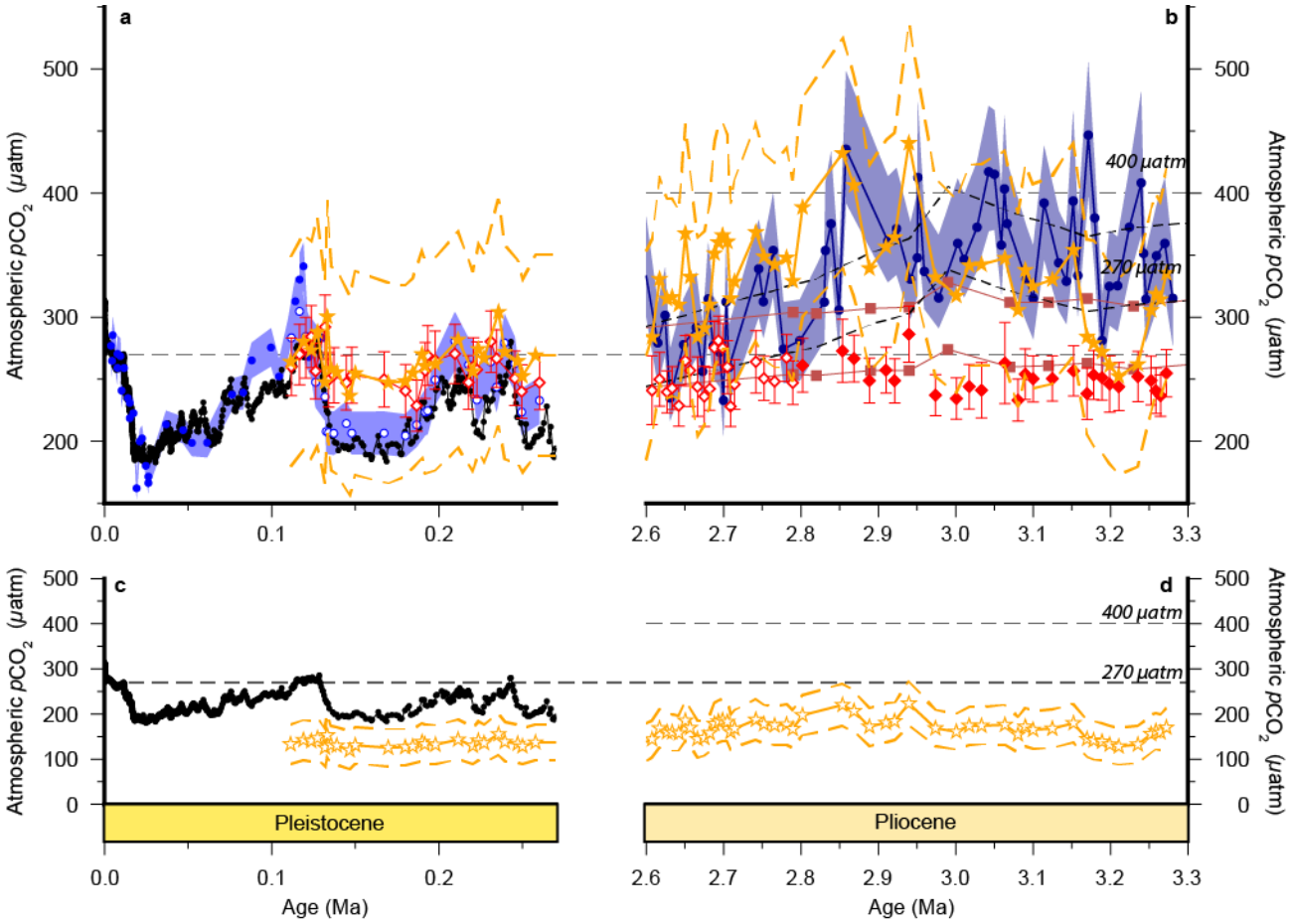

Figure 6 Cell size corrections to $CO_{2(\varepsilon p\text{-}alk)}$. Ornamentation is the same as Figure 1, with the addition of cell size corrected $CO_{2(\varepsilon p\text{-}alk)}$. The smaller liths than modern *E. huxleyii* across all of our records of our records mean that a direct application of the method of Henderiks and Pagani (2007) result in substantially lower $CO_{2(\varepsilon p\text{-}alk)}$ throughout (orange open stars, panels c,d). As the main interest is in the effect of the Plio-pleistocene change in cell size we observe, we adjusted the b' term so that $CO_{2(\varepsilon p\text{-}alk)}$ matched our uncorrected $CO_{2(\varepsilon p\text{-}alk)}$ record during the last interglacial (orange filled stars, panals a,b).

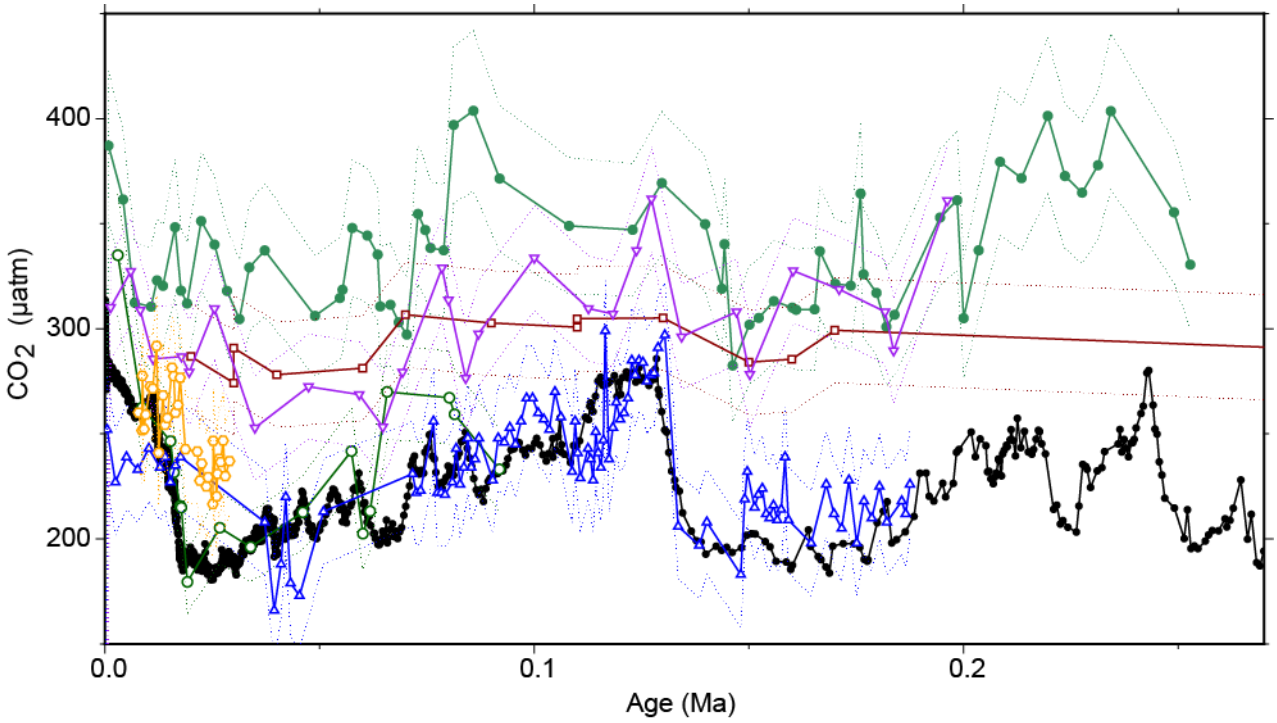

Figure 7~~6~~ Recalculated $CO_{2(\varepsilon p\text{-}alk)}$. Previous work (Jasper et al., 1994; Jasper and Hayes, 1990) **calculated $CO_{2(\varepsilon p\text{-}alk)}$ using a different model; here we recalculate the earlier work using the modern methodology and Monte Carlo propagation applied to our other sites. All previous records have been recalculated using the same methodology as our new record, with some corrections and adjustments (for example for growth rate or lith size) removed to allow direct comparisons. Records are from MANOP Site C from the central equatorial Pacific (0° 57.2' N, 138° 57.3 W; green filled circles;** Jasper et al., 1994)**, DSDP Site 619 in the Pigmy Basin, northern Gulf of Mexico (27° 11.6'N, 91°24.5'W; green open circles** Jasper and Hayes, 1990)**, site 05PC-21 from the Japan Sea (38.40 °N, 131,55 °E; blue open triangles, (**Bae et al., 2015)**, site NIOP464 in the Arabian Sea (22.15 °N, 63.35 °E; orange open hexagons (**Palmer et al., 2010)**, site GeoB 1016-3 in the Angola Current (11.59 °S, 11.70 °E, purple inverted triangles (**Andersen et al., 1999) **and ODP Site 925 (4° 12.25' N. 43°,29.33' W; dark red open squares,** (Zhang et al., 2013)**.~~MANOP Site C from the central equatorial Pacific (0° 57.2' N, 138° 57.3 W) is shown as green filled squares~~circles~~, DSDP Site 619 in the Pigmy Basin, northern Gulf of Mexico (27° 11.6'N, 91°24.5'W) is shown as open squares, and ice~~ Ice **core data are shown as filled black circles and lines** (Bereiter et al., 2015 and Table 1)**. Dashed lines are 2σ uncertainties are from Monte Carlo error propagation as described elsewhere in the text. ~~Neither coccolith nor growth rate corrections were applied.~~**

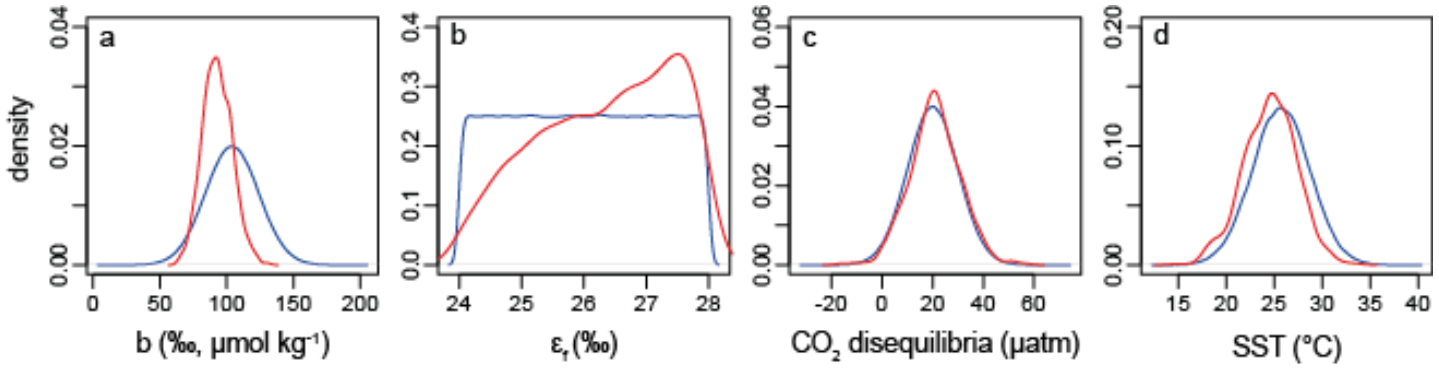

Figure 8~~7~~. Example of the Bayesian treatment of the $CO_{2(\varepsilon p\text{-}alk)}$ proxy, the sample shown is 0.15 Ma from ODP Site 999. In all panels the prior is shown in blue and the posterior in red. (a) the b-term, (b) ε_f, (c) the extent of CO_2 disequilibria, (d) sea surface temperature.

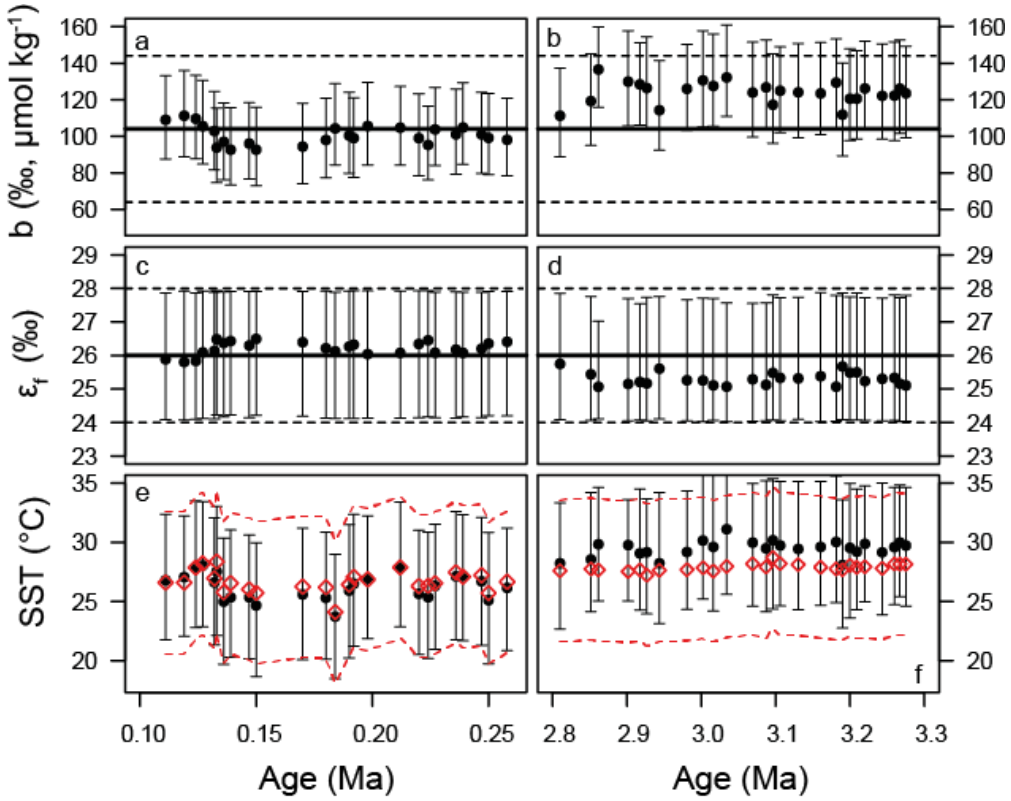

Figure 98. Timeseries of priors and posteriors for the b-term (a, b), ε_f (c,d) and SST (e,f). The Pleistocene is shown on the panels on the left and the Pliocene on the right. In panels a-d the mean of the prior distribution is shown as a thick black line. For the b-term 95% of the input distribution is shown as a dotted line, for ε_f the total range is shown. See Figure 7 for examples of these distributions as probability functions. For SST (e,f) the prior is shown as red diamonds with 95 % of the distribution shown as the dashed lines. In all panels the median of the posterior distributions are shown as circles with error bars encompassing 95 % of the range.

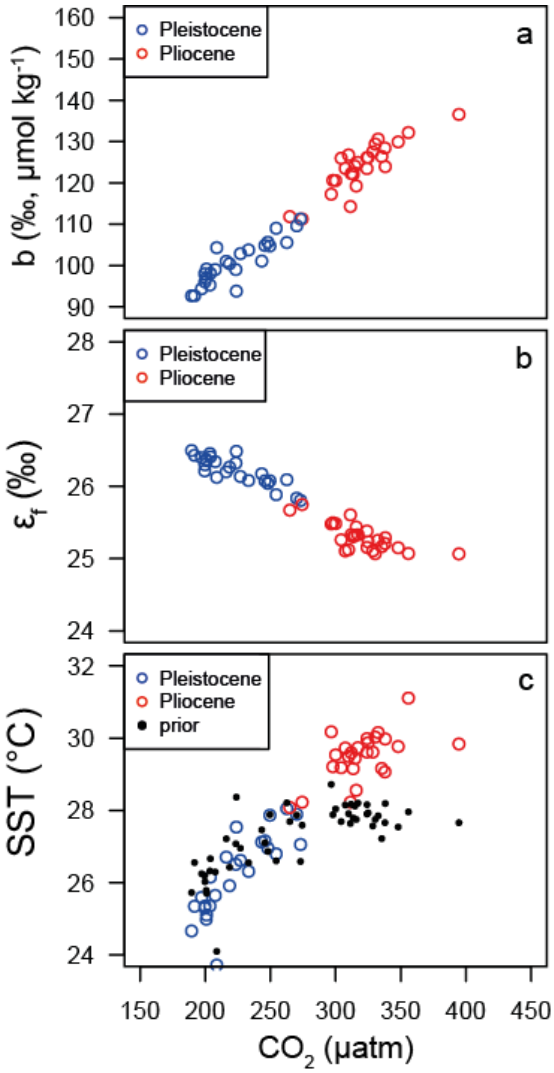

Figure 109. Relationships between CO_2 and (a) b-term, (b) ε_f and (c) SST. In each panel the median of each posterior distribution is shown in red for the Pliocene and blue for the Pleistocene. Note that the CO_2 for each data point is either from the ice core or $CO_{2(\delta 11Bplank)}$ for the Pleistocene and Pliocene, respectively. The linear patterns that emerge here essentially represent the relationships of the Bidigare et al., (1997) **approach given our otherwise invariant ε_p.**

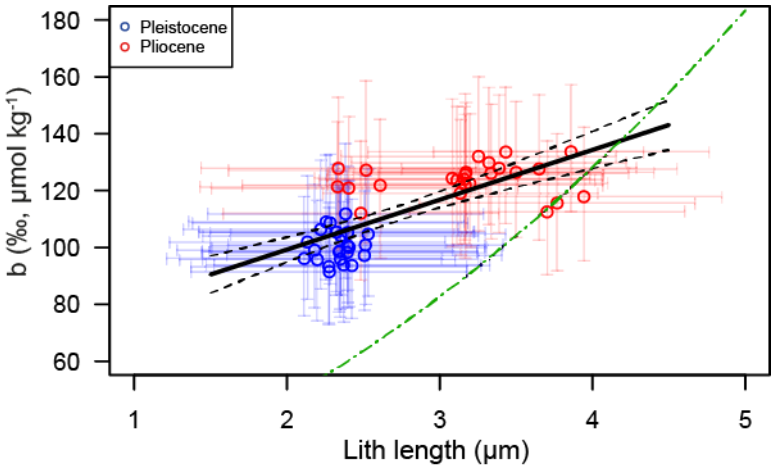

Figure 11. Comparison between the posterior distribution for the Pliocene (red circles) and Pleistocene (blue circles) and the lith size correction of (Henderiks and Pagani, (2007) **(green dot-dash line).**